# NUMERICAL SOLUTION OF THE NAVIER-STOKES EQUATIONS ABOUT THREE-DIMENSIONAL CONFIGURATIONS - A SURVEY

Terry L. Holst*
NASA Ames Research Center, Moffett Field, California

## Abstract

The numerical solution of the Navier-Stokes equations about three-dimensional configurations is reviewed. Formulational and computational requirements for the various Navier-Stokes approaches are examined for typical problems including the viscous flow field solution about a complete aerospace vehicle. Recent computed results, with experimental comparisons when available, are presented to highlight the presentation. The future of Navier-Stokes applications in three-dimensions is seen to be rapidly expanding across a broad front including internal and external flows, and flows across the entire speed regime from incompressible to hypersonic applications. Prospects for the future are described and recommendations for areas of concentrated research are indicated.

## Introduction

The fields of Computational Fluid Dynamics (CFD) and computer hardware design have been rapidly advancing over the last decade. It is now possible to demonstrate the importance of CFD in the field of aircraft design and performance prediction for general flow conditions including reasonably complete viscous effects. The problem of solving the Navier-Stokes equations about complex three-dimensional geometries has been undertaken and significant results have already been produced. The purpose of this paper is to review the current status of CFD applications in this area and to give prospects for the future especially for those applications involving complex geometries. Computational requirements for producing these results both now and in the future will be addressed.

The first pioneering calculations with the Navier-Stokes equations generally involved turbulent solutions with simple algebraic turbulence models (or laminar solutions with no turbulence models) in two dimensions with generally simple geometric shapes. These aspects were required to eliminate the complexity of turbulence and to reduce computational requirements to fit the computational facilities that existed in the early and mid 1970s. A good review of early work in this area is given by Peyret and Viviand.[1] Several years after the first two-dimensional Navier-Stokes solutions appeared, three-dimensional simulations were presented, again using algebraic turbulence models (or a laminar flow assumption) and simple geometries. Since then improvements in computers and algorithms have allowed tremendous advances in CFD across a broad front of different applications.

The rate of increase in the number and size of three-dimensional Navier-Stokes simulations is displayed in Fig. 1. This figure shows grid size for a representative sample of three-dimensional Navier-Stokes simulations plotted versus the year the results were published. Several observations are immediately obvious. The first three-dimensional simulations did not start appearing until the mid-1970's and since then the growth in both number and size of simulations has been almost exponential. This trend is due to improved algorithms, faster computers with larger main memories and to the availability of more computer time. The approximate cost of these computations can be inferred from Fig. 2 where the number of operations is plotted versus grid size. Note that the speed regime associated with each computation ranging from incompressible to hypersonic is also indicated. The solid line is an estimate of projected growth that appeared in Ref. 2 in 1983. This estimate was based on only the studies available in the pre-1983 time frame, and yet the curve represents a reasonablly valid trend. Actually, the number of operations required to obtain a solution for the finer grids is somewhat underpredicted by this estimate. This is probably due to additional "stiffness" associated with finer grids and the fact that these solutions are newer and therefore probably less efficient.

This survey is divided into several sections listed as follows: CFD Formulations, where the major governing equations used in CFD are described with special emphasis on the Navier-Stokes formulation; Previous Survey Work, where past surveys are listed; Status of Navier-Stokes CFD, where Navier-Stokes CFD is surveyed including the areas of incompressible flow, transonic flow, supersonic/hypersonic flow and high-alpha/vortex-dominated flow; and Concluding Remarks. Because of the breadth associated with this review and the Navier-Stokes CFD

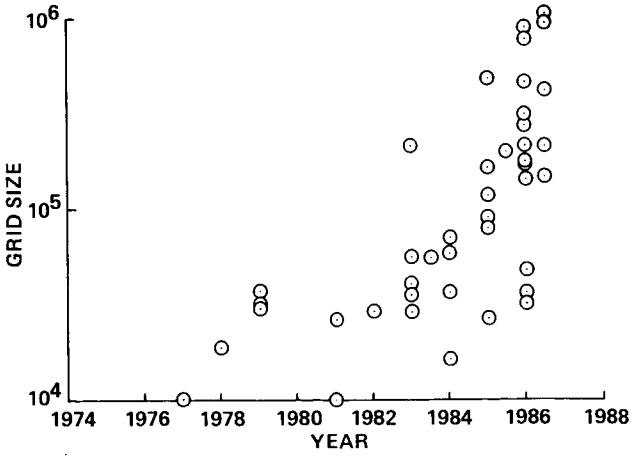


Fig. 1. Growth in the number and size of three-dimensional Navier-Stokes simulations using the time-asymptotic approach to obtain steady solutions.

* Chief, Applied Computational Fluids Branch.



C-4

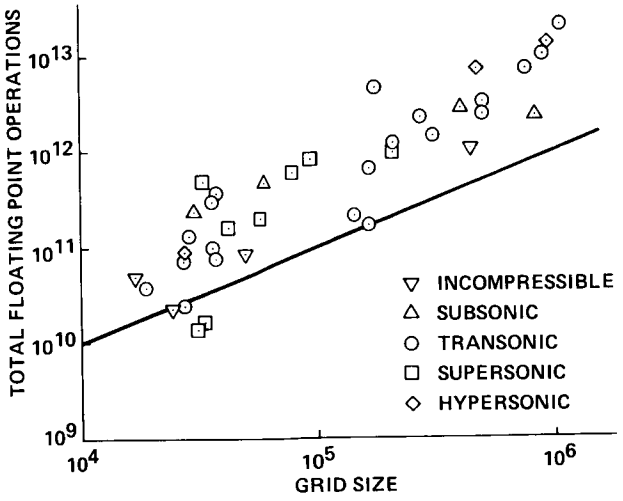


Fig. 2. Estimated floating-point operations required for a converged solution as a function of grid size for selected three-dimensional time-asymptotic RANS solutions.

field in particular, no claim of completeness is made nor should one be assumed. The first item for discussion is how the Navier-Stokes formulation, and in particular, the Reynolds-Averaged Navier-Stokes (RANS) formulation, fits into all the other CFD formulations.

## CFD Formulations

The aforementioned improvements in computer execution speed and main memory capacity achieved in the past several years has made it possible to dramatically expand the field of CFD. This has resulted in significant progress up the hierarchal "ladder" of CFD formulation complexity as shown in Fig. 3. Panel method solutions, which effectively solve the linear Laplace equation using the principle of superposition, have been studied thoroughly during the past three decades. As a result, panel method computer codes are well established within industry as efficient and reliable design tools for aircraft in the subsonic and supersonic speed regimes.

The next rung on the CFD formulational ladder is occupied by nonlinear potential formulations including the transonic small-disturbance and full potential equations. Both of these formulations have been extensively studied for the past 15 years and except for some grid generation limitations associated with complex geometry applications, these methods are well developed and heavily utilized within the aircraft industry design environment. Of course, these potential methods extend the range of applicability of CFD to the transonic speed regime and therefore have the capability of capturing weak shock waves and wave-drag levels. Appropriate reviews of this area can be found in Refs. 3 and 4.

The Euler equation formulation, which occupies the next rung on the CFD formulational ladder, is currently at the center of research in the Aerospace CFD community. New algorithms and applications in three dimensions

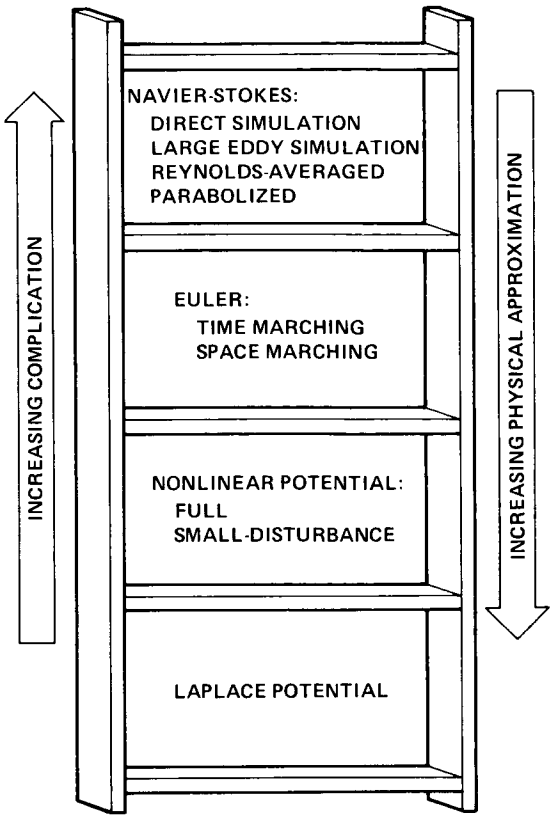


Fig. 3. Computational Fluid Dynamics formulational ladder.

have proliferated at a very fast rate in the past five years. The various design groups within industry have already started using Euler codes for many applications but significant improvements in code and/or computer efficiency have to be realized before the Euler formulation will be used extensively. The Euler formulation provides better accuracy for strong shock calculations and has the ability to properly track vorticity gradients. These features are important for a variety of advanced flow field situations including vortical aerodynamic studies, strong shock calculations, high angle-of-attack leading-edge flow separation, high-speed blunt body problems, and blast wave studies.

The highest entry on the CFD formulational ladder is occupied by the Navier-Stokes equations. This formulation is the most complex and represents the smallest level of physical approximation. Like the Euler formulation, much work has been completed in the three-dimensional Navier-Stokes area during the past five years. However, the application of typical Navier-Stokes computer codes in the industry design environment has been slow to evolve. This is largely due to two reasons: First, the Navier-Stokes equations are several times more expensive to solve (at least) than the Euler equations. This is due to more terms in the Navier-Stokes equations; more grid points required to resolve a given problem, because in addition to the inviscid region, the boundary layer has to be resolved; and in separated flow cases, more iterations are required to achieve convergence because of the more complicated vis-

cous/inviscid interaction. The second major reason that the Navier-Stokes equations have not been used in design applications is due to the complications of turbulence. To discuss this subject a further breakdown of the Navier-Stokes formulation is required.

The Navier-Stokes equations intimately describe the motion of most fluid flow phenomena including large scale motions associated with the inviscid features of a flow field and small scale motions associated with turbulence. The numerical procedure which directly solves the Navier-Stokes equations and resolves all flow length scales including the smallest turbulent length scales is called direct simulation (DS). When the numerical grid resolution is not capable of resolving all length scales problems occur. Because for high Reynolds number flow the range of length scales is so immense, it is not currently possible to simulate this type of flow with schemes based on the DS approach. Thus, the first level of approximation to the Navier-Stokes equations, called Large Eddy Simulation (LES), is introduced. In the LES formulation the Navier-Stokes equations are solved on a grid which is capable of resolving all length scales except the smallest turbulent length scales. These length scales are associated with the smallest turbulent eddies in the flow field. Because these smallest eddies tend to be isotropic, they are easier to model than the larger eddies which tend to be random and can vary in nature for different flow conditions. A good review of the DS and LES areas is given in Ref. 5.

The LES formulation is still quite expensive and is restricted to problems with limited geometrical complexity and to moderate and low Reynolds numbers. This leads to the Reynolds-averaged Navier-Stokes (RANS) formulation where all turbulent eddies are modeled. The RANS formulation is derived by decomposing all dependent variables, e.g., density, pressure, and velocity components, into two parts, a mean part and an unsteady part. The unsteady part contains the unsteadiness due to high-frequency turbulent fluctuations and the mean part contains the average local flow value for that variable including any low-frequency time variation. After this variable decomposition process the resulting Navier-Stokes equations are time averaged over a time scale which is large in comparison with turbulent fluctuations but small in comparison with mean flow field unsteadiness. As a result of the time-averaging process, certain new terms arising from turbulent eddy correlations remain. These new terms account for the mean or average effect of turbulence and must be modeled. This allows the numerical solution of the Navier-Stokes equations for many applications involving realistic Reynolds numbers on grids that will fit on existing supercomputers.

One variation of the RANS equations first suggested by Baldwin and Lomax[6] and used in a variety of applications, is the so-called "thin-layer" formulation. This formulation requires a no-slip boundary surface to be aligned with a constant coordinate surface, which is a typical facet in most applications. The thin-layer formulation is obtained by dropping all viscous terms containing transverse spatial derivatives. The justification for this assumption is that these terms are typically small in most regions of flow and that in regions where they are potentially large, for example, near separation, grid resolution is not generally adequate to resolve them. In addition, numerical experimentation using both the full and thin-layer forms has shown little or no difference in the computed results, and the thin-layer formulation is approximately 30% cheaper. It should be stressed that although the thin-layer Navier-Stokes assumptions are similar to certain classical boundary layer assumptions, the resulting equations are quite different. All time terms are retained, that is, the thin-layer Navier-Stokes equations are still hyperbolic, while the boundary layer equations are parabolic. Thus, the thin-layer Navier-Stokes formulation has no numerical difficulty with either streamwise or cross-flow separations.

The last Navier-Stokes formulation discussed here is the Parabolized Navier-Stokes (PNS) formulation. This formulation is derived from the RANS equations and therefore requires the modeling of all turbulent length scales. The PNS approach also requires the flow to be supersonic in the streamwise direction (although under certain conditions when the pressure field is specified the freestream can be subsonic) and that there be no streamwise separations in the boundary layer. In addition, all time-dependent terms and streamwise diffusion terms are neglected. Under these assumptions the Navier-Stokes equations become parabolic in the streamwise direction and can be solved numerically using a space-marching procedure instead of the standard time-asymptotic approach. Thus, the computer requirements (both memory and cpu time) are much less demanding for the PNS approach relative to the time-dependent approach.

A comparison of the estimated memory and execution time requirements for several different formulations is given in Fig. 4. An additional horizontal scale indicates the amount of execution time required by a theoretical gigaflop computer, which should be available in the near-term future. This figure was constructed from information given in Refs. 7-11. The Euler formulation and three of the Navier-Stokes formulations just discussed (DS, LES, and RANS) are all included. Note that several variations of the RANS formulation (steady ideal gas, steady nonequilibrium real gas, and unsteady ideal gas) are presented. Including nonequilibrium real gas effects associated with hypersonic flight or the unsteadiness effects associated with (for example) high-alpha flight, may increase the computational costs of a typical steady RANS calculation by an order of magnitude. This additional expense while prohibitive today may not be prohibitive in the near-term future.

The prospects of computing three-dimensional flows at realistic flight Reynolds numbers using the LES formulation in the near future do not seem bright. As indicated in Fig. 4 the cpu time for such a calculation on a theoretical gigaflop computer would be on the order of one month. The DS picture is even more dismal with cpu times for a single three-dimensional calculation requiring on the order

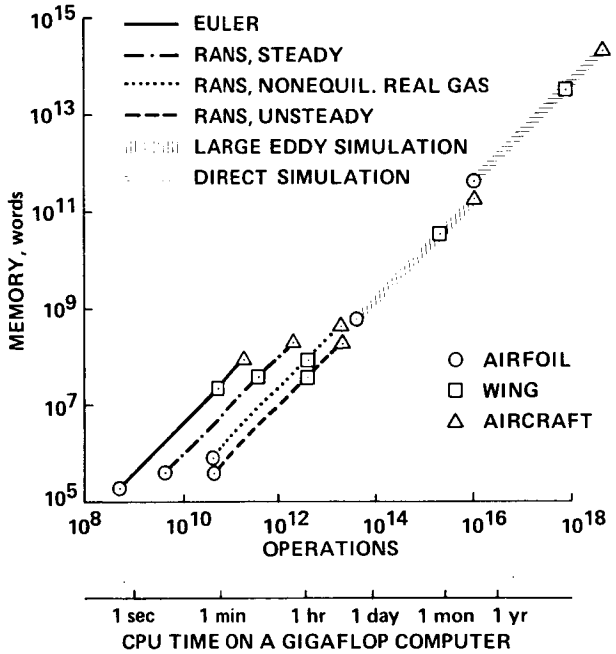


Fig. 4. Estimated memory and execution time requirements for several different CFD formulations.

of years. Hence, it seems that the most appropriate Navier-Stokes formulations for attention in the area of applications involving realistic Reynolds numbers and reasonably complex geometries, are the time-dependent RANS and PNS formulations. The remainder of this survey will be solely devoted to these areas with primary emphasis on the time-dependent RANS formulation. For an indepth technical discussion of most of the CFD formulations just discussed, the interested reader is referred to Ref. 12.

## Previous Survey Work

Several interesting surveys on the subject of Computational Aerodynamics have been produced recently. Two particularly important articles are from Chapman[11,13] where the entire field of Computational Aerodynamics is reviewed; pacing items including turbulence modeling, three-dimensional grid generation, algorithm development, and computer speed limitations are discussed in detail; and computational requirements and projected computer capabilities are examined. More recent surveys along the same line are by Kutler.[10,14] The same critical pacing items are examined and updated.

Other pertinent reviews in the area of CFD are by Shang[15] where the RANS formulation is discussed for various geometric applications, Mehta and Lomax[16] where the RANS formulation for transonic flow is discussed with special emphasis on algorithmic details and aspects of turbulent physics, Chaussee[17] where the PNS approach is described with special emphasis on applications, Orszag and Israeli[18] where early work associated with the solution of the incompressible Navier-Stokes equations is reviewed, and Turkel[19] where computational physics is reviewed with emphasis on algorithms and convergence acceleration. Additional areas related to the numerical solution of the Navier-Stokes equations are grid generation, which is reviewed in detail by Thompson,[20] and turbulence modeling, which is described with particular emphasis on three-dimensional flows involving curvature, separation, and vorticies, by Lakshminarayana.[21]

An important aspect associated with CFD research is the area of experimental fluids research. A good review in this area is given by Marvin[22] where CFD code verification experiments are described and in Ref. 2 where the projected influence of CFD on experimental facilities is discussed. Of course, the influence of the experimental world on CFD has been profound. The opposite is also true, CFD has begun to influence the experimental world as well. The CFD field has generated the need to conduct a whole new series of experiments to validate CFD code results.[22] These experiments generally take advantage of the latest developments in sophisticated measurement techniques and generally get more involved with fundamental flow phenomena. Having intimate CFD/experimental interaction is an important feature and must remain as an essential ingredient in CFD research, especially in areas involving unexplained flow phenomena such as shock-induced or angle-of-attack induced flow separation.

Before proceeding with the main emphasis of this review, an additional statement regarding experimental validation of numerical solutions is in order. A typical steady three-dimensional Navier-Stokes solution produced today consists of 100,000-200,000 grid points each with 5 dependent variables resulting in a total data base of perhaps one million words for each set of free-stream conditions. Corresponding experimental data bases, not counting qualitative flow visualization results, generally consist of perhaps only a few hundred data points for each set of free-stream conditions. These data are usually in the form of surface pressures. This general lack of extensive data, including interior flow field data, makes thorough validation of CFD results difficult. If the experimental and computational surface pressures agree, this by no means requires other aspects of the flow field to agree. If the surface pressures disagree, the physical reasons for this disagreement are usually not apparent. Thus, it is imperative that sufficient detail associated with CFD validation experiments be obtained to fully evaluate numerical results and to provide the maximun understanding of basic fluid flow phenomena.

## Status of RANS/PNS CFD

This survey is divided into several different areas of application as follows: incompressible flow, transonic flow, supersonic/hypersonic flow, and high-alpha/vortex-dominated flow. The first two areas will be limited to time-dependent RANS applications and the latter two will include both time-dependent RANS and PNS applications. All the research surveyed will be restricted to three spatial dimensions and most of the applications will be associated with steady flow. First, the discussion centers on

the numerical solution of the Navier-Stokes equations for incompressible flow.

## Incompressible Flow Applications

Numerical solution of the incompressible Navier-Stokes (INS) equations in three dimensions has received much attention during the past several years. In the study of incompressible flow algorithms, it is interesting to study compressible algorithms and the connections between the two fields. The overwhelming majority of all steady compressible algorithms applied to flows that are partially or totally subsonic outside the boundary layer, utilize a time-accurate or time-like iteration to asymptotically approach steady-state solutions with increasing time. The application of this approach to incompressible problems is difficult because of the basic difference in incompressible and compressible continuity equations. The incompressible continuity equation is the familiar condition that requires the divergence of the velocity vector to vanish. Thus, there is no time-dependent term as with the compressible continuity equation. Also associated with this problem is the lack of an explicit relation for the pressure. These two features cause the primary difference between incompressible and compressible algorithms. Note: Certain two-dimensional algorithms, for example, stream-function/vorticity schemes, deal with these difficulties quite nicely but are difficult to extend to three dimensions, and therefore, will not be discussed further.

Early numerical work in the incompressible flow area was presented by Harlow and Welch,[23] Chorin,[24] and Patankar and Spalding[25] where three basically different approaches were presented. In the first approach, a Poisson equation for the pressure was derived by taking the divergence of the momentum equation. This equation is then solved iteratively using the velocity field at time level n to predict the pressure such that the continuity equation is satisfied at time level n+1. This process is time accurate and can be continued until a steady-state solution is reached. Needless to say, because of the additional iteration required to solve the pressure Poisson equation, this method is computationally expensive.

In the second approach, the method of artificial compressibility was introduced. An artificial time-dependent pressure term is added to the steady continuity equation which allows the resulting equations to be solved using standard time-dependent compressible algorithms. As the solution converges, the time-dependent pressure term is driven to zero and the flow approaches the incompressible limit. In the last approach, a space marching procedure was developed by reducing the incompressible Navier-Stokes equations to a set of parabolic equations. The pressures are determined by first computing the velocities from estimated pressures, then a correction is applied to the pressure so as to satisfy the continuity equation. Of course, the latter approach does not work successfully if streamwise flow separation occurs.

More recent work in the area of INS solvers has been presented in Refs. 26-32 where three-dimensional ducts with curvature were considered for a wide variety of flow conditions, Himeno et al.[33] where the wake structure downstream of various bluff bodies was computed using the INS method described by Kawamura and Kuwahara,[34] Kwak et al.[35] where a variety of applications were reported including a rectangular duct flow with a 45 deg bend, Gorski et al.[36] where turbulent corner flows were presented using two different turbulence models, and Refs. 37-41 where various internal elements of the Space Shuttle Main Engine were analyzed. The algorithm used in Refs. 37-41 was the method of pseduo compressibility devised by Chang and Kwak.[42] This method is similar to Chorin's artificial compressibility method and is an outgrowth of the work of Steger and Kutler.[43] A recent upgrade to this algorithm was presented by Rogers et al.[44] where the original block-matrix ADI algorithm has been diagonalized to yield a scalar-matrix ADI algorithm which is about three times faster.

A typical incompressible flow result showing particle traces downstream of a circular-cylinder post mounted on a flat plate is displayed in Fig. 5 (taken from Ref. 40). This calculation is laminar with a Reynolds number of 1000. Note the formation of a saddle point of separation forward of the post and a horseshoe vortex downstream of the post. The secondary flow in front of the post wraps around the post and forms a "tornado-like" vortical flow in the wake of the post, which is strikingly different than the flow downstream of a simple post in the absence of the flat plate. An oil-flow photograph appearing in Ref. 40 provides qualitative validation for this type of vortical wake flow.

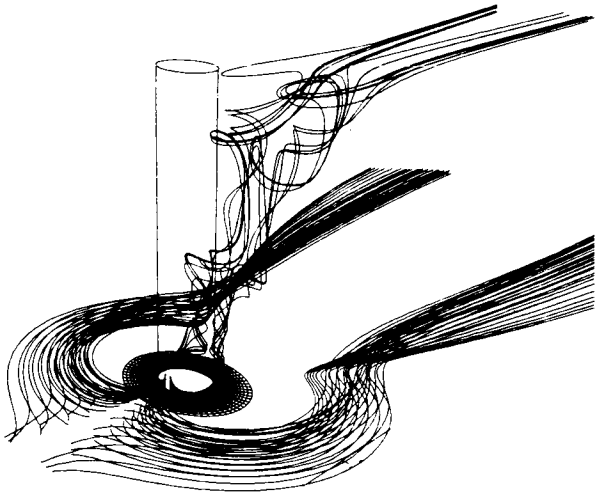

Fig. 5. Computed three-dimensional particle paths around and downstream of a circular-cylinder post mounted on a flat plate, incompressible flow, $Re = 1000$, Kwak et al.[40]

## Transonic Flow Applications

The transonic flow area has perhaps received the widest attention during the past five years in the three-dimensional RANS research community. In this area there are a whole host of unsolved and interesting research topics that have practical applications for both commercial and military circles. A few of these include shock/boundary-layer interation including boundary-layer separation effects, wing/fuselage interference, performance prediction especially drag prediction, afterbody boundary-layer separation, and helicopter rotor-tip transonic performance.

Literally all transonic numerical methods for the Navier-Stokes equations utilize time-dependent formulations to obtain steady-state solutions asymptotically with increasing time. The time-integration algorithms used to implement this strategy vary from application to application. Most schemes utilize implicit methods, for example, the Beam-Warming,[45] Briley-McDonald,[46] or MacCormack[47] methods, or algorithms with suitable convergence acceleration, for example, multigrid. This theoretically allows large time steps to be taken, and therefore, provides rapid approach to the desired asymptotic solution. This philosophy works well but requires several hundred to several thousand iterations to produce acceptable levels of "convergence." The number of iterations generally increases as the mesh is refined and as the physics of the problem becomes more difficult, that is, stronger shock waves, larger separations, etc. Time-step limitations due to nonlinear numerical instabilities are common. This allows explicit time-integration methods, for example, MacCormack,[48] which generally have quite severe time-step limitations but which are cheaper per iteration and easier to code, to be appropriate alternatives for some applications.

The problem which has received the most attention in the transonic flow area is wing flow-field prediction. The first calculation of this type was presented by Mansour[49] where the RANS formulation was solved for the flow field about "Wing C" (defined in Ref. 50). The numerical scheme used in this study was a fully-implicit, ADI-like scheme developed by Beam and Warming[45] and Briley and McDonald[46] and first demonstrated in three dimensions by Pulliam and Steger.[51] The grid used in this study, while having an efficient topology, was coarse and produced only fair agreement with experiment. Another similar calculation for transonic wing geometries was presented by Agarwal and Deese.[52] In this study the explicit Runge-Kutta scheme of Jameson et al.[53] was extended to handle the RANS equations for the transonic flow about the ONERA-M6 wing (defined in Ref. 54). The grid was again coarse, but for the simple calculations reported (attached and nonlifting), the experimental/computational agreement was good.

More recent transonic RANS calculations for wing geometries have been given by Holst et al.,[55] Flores,[56] Kaynak et al.,[57,58] and Srinivasan et al.[59] These studies have utilized a computer program called TNS (Transonic Navier-Stokes) which uses the diagonalized-implicit algorithm of Pulliam and Chaussee[60] coupled with a zonal grid arrangement to solve the thin-layer form of the RANS equations. In addition, the Baldwin-Lomax turbulence model[6] was used in each case. In the TNS approach for grid zones near the wing surface, the RANS equations are solved and for zones away from the wing surface, where viscous terms are not important, the Euler equations are solved. In Holst et al.[55] solutions are presented for a low-aspect-ratio wing derived from the NACA 0012 airfoil section. Comparisons with the experimental data of Lockman and Seegmiller[61] for this wing at various transonic flow conditions including cases with shock/boundary-layer separation are presented and discussed. A significant aspect of this set of calculations is that the wind tunnel walls are very important and must be modeled to obtain good agreement with experiment. Generally good agreement was obtained when the walls were modeled and the flow was attached. For separated cases the agreement was not good, and this was attributed to the lack of proper grid refinement and inappropriate turbulence modeling.

Computed pressures produced by Kaynak et al.[57,58] for the previously discussed Wing C geometry are compared with experimental results from two sources, Hinson and Burdges[50] and Keener,[62,63] in Fig. 6. The free-stream Mach number for this set of results is 0.85, the angle of attack is 5 deg, and the Reynolds number is 8 million. The computed and experimental results are in good agreement; as much scatter between the two experimental results exists as between the computed and experimental results. Figure 7 shows the computed particle paths on the wing surface for the same case. Note the small shock-induced separation near the wing tip which is generally in good agreement with the corresponding experimentally produced oil flow pattern. Detailed computational/experimental comparisons for other cases are also presented in Kaynak et al.[57,58]

The computed results presented by Srinivasan et al.[59] also deal with the Wing C geometry as well as various helicopter rotor geometries. The main emphasis in this study is on tip vortex formation. With this purpose in mind special grid clustering at the wing tip was used. Computed particle paths on the surface of an ONERA wing designed to represent a typical helicopter rotor blade, are shown in Fig. 8. For this calculation the free-stream Mach number was 0.85, the angle of attack was 5 deg, and the Reynolds number was 8.5 million. A strong transonic shock wave near mid chord causes a large region of separated flow as shown in Fig. 8. An outward spiralling vortex emanates from the separated flow region near the tip. This can be seen in Figs. 9 and 10, which show standard and close-up views, respectively, of computed three-dimensional particle paths about the tip. As explained by Srinivasan et al.,[59] the cross flow created by the tip sweep enables the fluid particles released in the vincinity of the tip to first braid and then roll up and lift off of the surface.

Other notable transonic wing calculations are presented by Obayashi and Fujii[64] and Fujii and Obayashi.[65] In the later case high-aspect-ratio transport-type-wing flow fields are obtained using a new LU-ADI algorithm. This algorithm utilizes the flux vector splitting technique

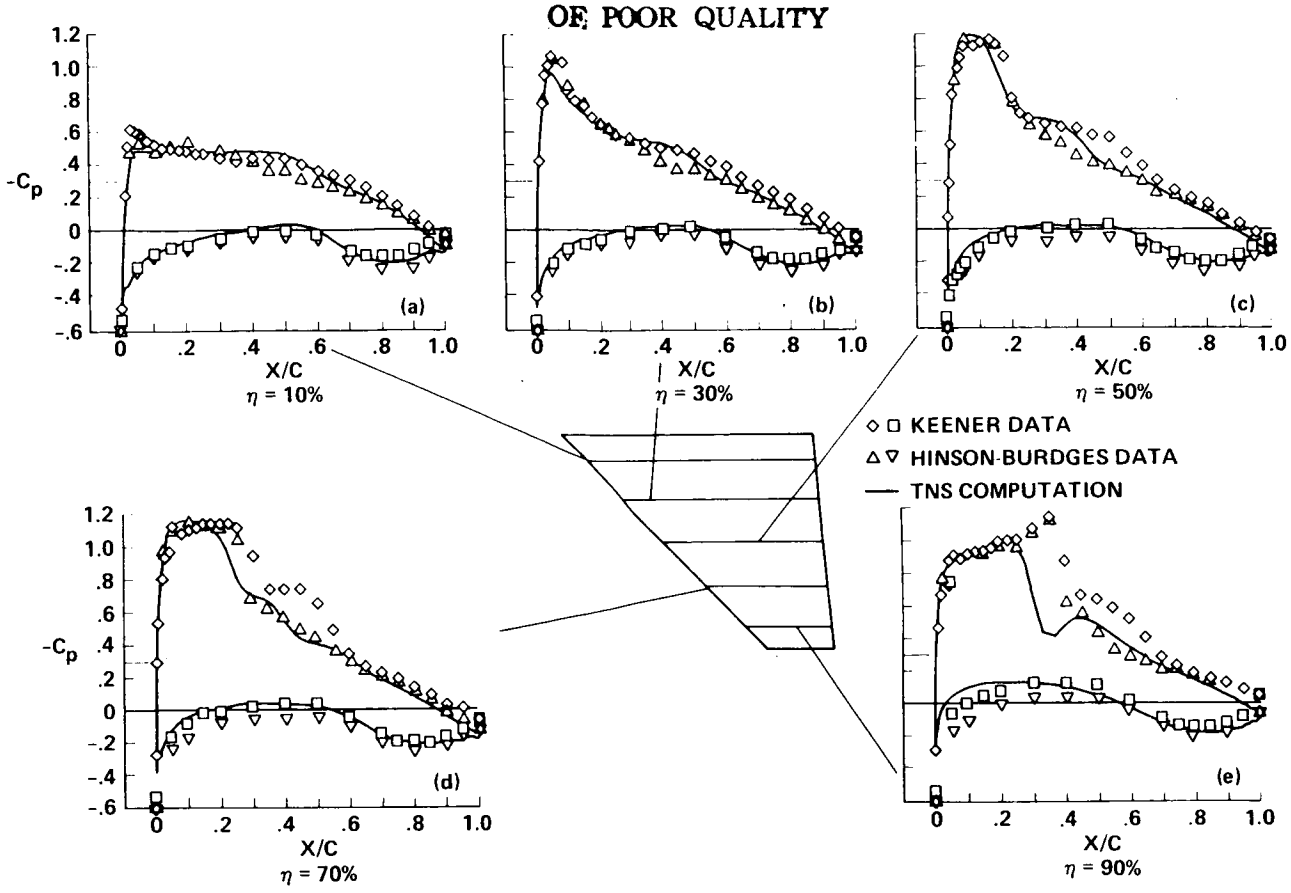


Fig. 6. Pressure coefficient comparisons for the "Wing C" geometry, $M_\infty = 0.85$, $\alpha = 5°$, $Re = 8\text{x}10^6$, Kaynak et al.[58]

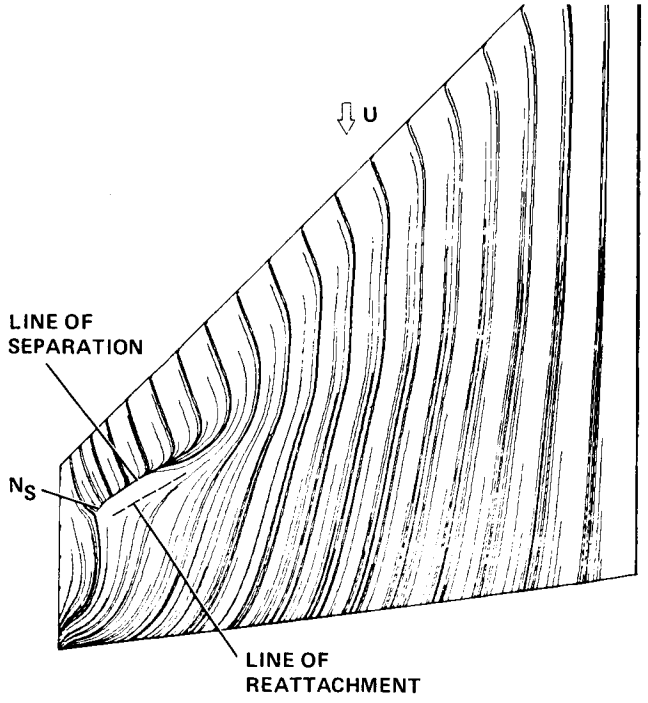


Fig. 7. Computed surface particle paths for the "Wing C" geometry, $M_\infty = 0.85$, $\alpha = 5°$, $Re = 8\text{x}10^6$, Kaynak et al.[58]

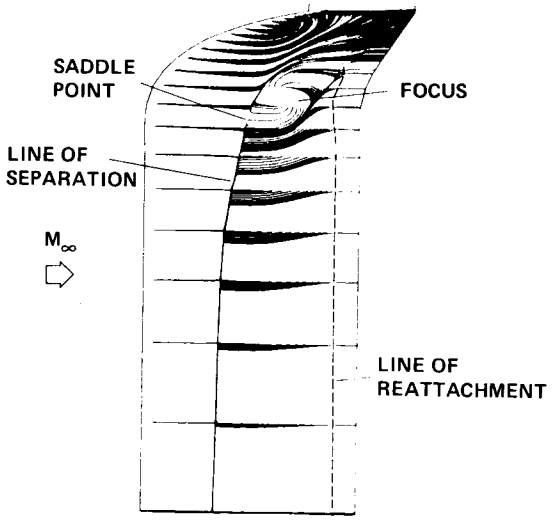


Fig. 8. Computed surface particle paths for a swept-tip helicopter blade, $M_\infty = 0.85$, $\alpha = 5°$, $Re = 8.5\text{x}10^6$, Srinivasan et al.[59]

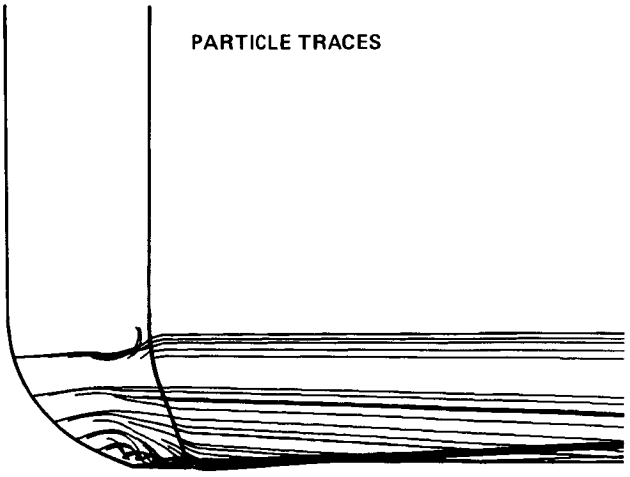


Fig. 9. Computed three-dimensional particle paths around a swept-tip helicopter blade, $M_\infty = 0.85$, $\alpha = 5°$, $Re = 8.5\text{x}10^6$, Srinivasan et al.[59]

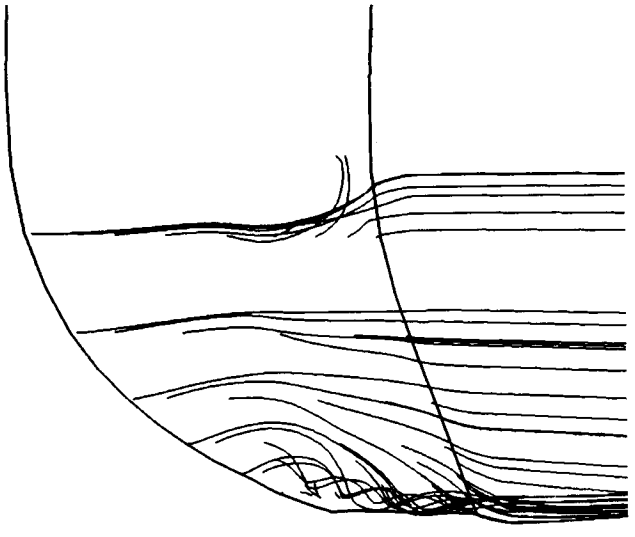

Fig. 10. Blow-up view of Fig. 9 showing tip flow-field detail, Srinivasan et al.[59]

of Steger and Warming[66] and the diagonally dominate factorization of Lombard et al.[67] to decompose the usual block tridiagonal system into the product of lower and upper scalar bidiagonal matricies. In this study flow fields with strong shock/boundary-layer interation and the resulting massive boundary layer separation are computed for a series of cases. Good correlations with experimentally measured pressures are presented.

The LU-ADI transonic wing method just discussed has also been extended to handle wing/fuselage geometries by Fujii and Obayashi.[68] A typical result from this study is shown in Figs. 11 and 12. This case invloves a high-aspect-ratio wing low-mounted on a transport-type fuselage. The Mach number, angle of attack, and Reynolds number for this solution are 0.82, 4.0 deg, and 1.67 million, respectively. Computed and experimental pressure distributions are compared in Fig. 11 and computed surface particle paths are shown in Fig. 12. Note the shock-induced separation at about mid chord and the wing-fuselage/juncture separation which is highlighted by a large spiral node on the aft-wing-root surface. This set of calculations is also quite unique due to the level of grid refinement used. For these calculations a grid of 119 x 71 x 92 = 777,308 points was used and represents the finest RANS grid with a published solution to date.

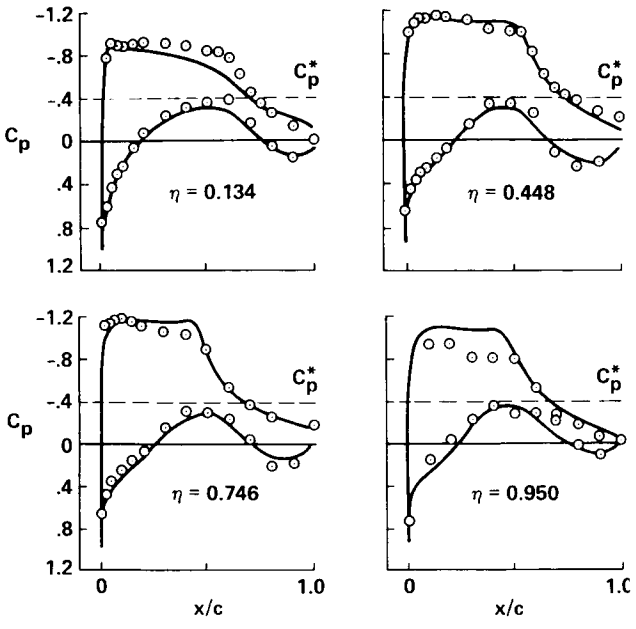


Fig. 11. Pressure coefficient comparisons for a high-aspect-ratio wing/fuselage configuration, $M_\infty = 0.82$, $\alpha = 4°$, $Re = 1.67\text{x}10^6$, Fujii and Obayashi.[68]

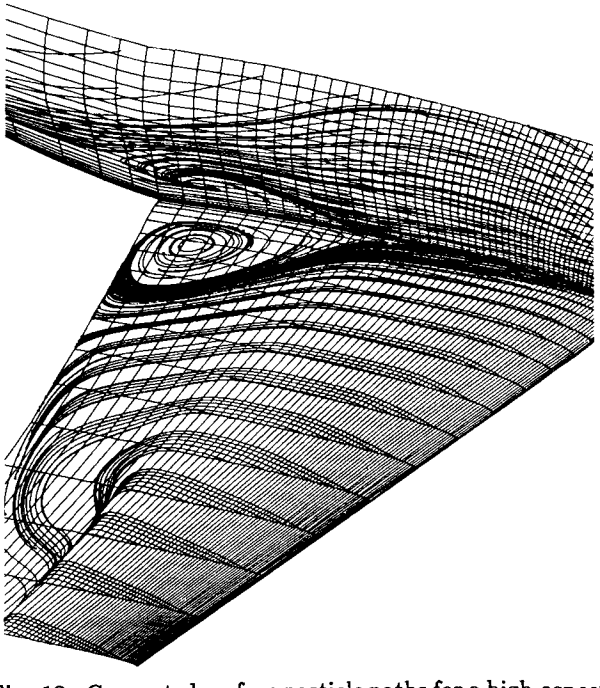

Fig. 12. Computed surface particle paths for a high-aspect-ratio wing-fuselage configuration, $M_\infty = 0.82$, $\alpha = 4°$, $Re = 1.67\text{x}10^6$, Fujii and Obayashi.[68]

Additional RANS calculations have been published for a wide variety of other types of transonic applications. These studies include the simulation of nacelle/inlet flow fields by Vadyak,[69] calculations through swept-blade cascades by Swisshelm and Johnson,[70] the simulation of forebody flow fields by Chaussee et al.[71] and Cosner,[72] the simulation of three-dimensional boattail afterbody flows by Deiwert,[73] and computations to determine the wake structure downstream of a three-dimensional turret by Purohit et al.[74,75] Another area with a lot of RANS research activity is transonic projectile aerodynamics. In this field the prediction of lift, drag, and magnus forces is very important and is intimately related to viscous effects. Interesting studies in this area include Nietubicz et al.[76] where the Magnus forces associated with a spinning projectile were first computed, Nietubicz et al.[77] where detailed computations to predict various aerodynamic coefficients were presented, and Sahu et al.[78] where the projectile base flow field was computed at transonic speeds. This group of studies, ranging from inlets to projectiles, used a variety of different integration schemes ranging from the classical explicit MacCormack[48] scheme to all types of implicit and multigrid schemes. The turbulence models used are largely dominated by the Baldwin-Lomax model[6] with all of the models being in the algebraic category. The more complicated one- and two-equation models have not generally found their way into three-dimensional transonic Navier-Stokes applications.

Supersonic/Hypersonic Flow Applications

Supersonic flow field solutions are somewhat easier to obtain relative to transonic flow fields. This is because the physics of supersonic flow typically allows smaller computational domains, the supersonic equation type is consistently hyperbolic (at least for inviscid regions) while for transonic flows the type is mixed between hyperbolic and elliptic, and the shock/boundary-layer interactions associated with supersonic flows are not as complicated as those associated with transonic flows. In addition, as already discussed, the supersonic free-stream characteristic allows the introduction of marching algorithms, that is, the PNS formulation. Hypersonic flows, while enjoying the same advantages of supersonic flow, contain other complications that even today have not been fully evaluated. These include more complicated transition and turbulence physics, real gas effects, merged shock and boundary layers, stronger shock waves, and radiation effects.

The field of supersonic CFD utilizing both the time-dependent Navier-Stokes and PNS formulations for computing three-dimensional applications has been widely researched in the past 6-8 years. Early pioneering Navier-Stokes calculations in this area include Li[79] where laminar flow separation on blunt flared cones at angle of attack was studied, Holst and Tannehill[80] where viscous blunt body flows with an impinging shock were studied, Shang and Hankey[81] and Hung and MacCormack[82] where the flow in a three-dimensional compression corner was solved, Hung[83] where the flow over an inclined body of revolution was obtained, Hung[84] where the impingement of an oblique shock wave on a cylinder was investigated, Knight[85] and Hung and MacCormack[86] where an oblique-shock/boundary-layer interaction flow field was simulated, and Hung and Kordulla[87] and Hung and Buning[88] where the flow about a blunt-fin/flat-plate interaction was computed. The Mach number for these calculations ranged from low supersonic to hypersonic with the maximum being 12.5. About half of the calculations, especially the eariler ones, were laminar, and the other half were turbulent with a variation of the Baldwin-Lomax turbulence model used in all cases.

As seen in the previous examples, turbulence modeling associated with the three-dimensional RANS formulation has not reached a very sophisticated level. For attached flow cases, existing algebraic, or "zero-equation" models as they are formally called, seem to do a good job for a wide variety of circumstances. When the flow experiences moderate or massive separation, these models do a poor job. For example, the most commonly used turbulence model is the Baldwin-Lomax model, which tends to underpredict the level and height of reversed flow in separation regions. This is probably due to an effective overprediction of dissipation in reqions of separated flow. More sophisticated models of the so-called one- or two-equation variety seem to improve the correlation in some cases while making it worse in others. Two difficulties associated with their use are additional complication, that is, new differential equations have to be solved, and additional numerical stiffness which causes the need for more flow solver iterations. Because of this lack of a clear direction and because of the additional complication, movement to use these more sophisticated turbulence models in three-dimensional applications has been slow.

Additional supersonic Navier-Stokes calculations are given by Horstman et al.[89] for swept compression corners and axisymmetric bodies with either skewed or segmented conical flares; Horstman[90] for swept compression corner flows; and Knight,[91] Knight et al.,[92] and Horstman[93] for swept-shock-wave/boundary-layer interaction studies. All of these three-dimensional computations involved Mach 3 flows with significant shock-induced boundary layer separation. In addition, most of these studies utilize some form of the more sophisticated two-equation $k$-$\epsilon$ eddy-viscosity turbulence model. In Ref. 92 computations with both the Baldwin-Lomax algebraic model and the Jones-Launder[94] two-equation model were performed. The Jones-Launder computations also utilized Viegas-Rubesin[95] wall function boundary conditions which permit the use of coarse grids in the lower portion of the boundary layer. This reduces the amount of computer time required for a converged solution. Results from Ref. 92 indicate that, at least for the swept-shock/boundary-layer interaction flows studied, the overall structure of the three-dimensional flow was insensitive to the turbulence model, except within a small portion of the boundary layer near the surface.

The difficulties associated with obtaining good turbulence models for complex applications exists for all speed regimes. However, the problems associated with the hypersonic flow regime are the most severe. At hypersonic

speeds certain incompressible flow assumptions used in formulating turbulence models, which are still valid up to Mach numbers of about 5, start to break down. In addition, hypersonic flows, especially for Mach numbers well above 10, will have chemical reactions which may interact with the turbulence. For moderate to high altitudes, hypersonic flows will be transitional, further complicating the situation. It is clear that much work in the area of turbulence modeling in general, and for the hypersonic regime in particular, will be required in the near future.

Flow field computations about more complicated geometries have been explored in the supersonic/hypersonic flow regime. Examples of time-dependent RANS calculations in this area include Shang[96,97] where the hypersonic wing-fuselage interference problem was studied with two different grid topologies, Kumar[98] where the supersonic flow upstream and through a two-strut scramjet inlet was computed, Howlett and Hunter[99] where the supersonic flow around and inside an inlet with spiked centerbody was simulated, Rizk and Ben-Shmuel[100] where the low-supersonic flow field about the space shuttle orbiter was investigated, and Li[101] where the hypersonic flow about an aerobrake body was considered. Another significant study in this area is the work of Shang and Scherr.[102] In this paper the entire flow field over the X-24C Lifting Body at a Mach number of 5.95, an angle of attack of 6 deg, and a Reynolds number of 16.4 million/m was obtained with a time-dependent RANS approach. The computational grid was extremely fine, consisting of 475,200 points, and represented the finest-grid RANS solution published up to 1985. The explicit MacCormack numerical scheme was used and the turbulence was modeled with the Baldwin-Lomax model. A typical set of results from Ref. 102 is shown in Figs. 13-15. Figure 13 shows the surface streamline pattern over the lifting body and demonstrates the level of complication that can be captured with the RANS approach when fine grids are used. Pressure distributions are compared with experiment in Figs. 14 and 15. Figure 14 shows comparisons over the fore part of the lifting body and Fig. 15 comparisons over the aft part. For all stations the agreement is excellent.

An additional complex-geometry study performed by Deiwert and Rothmund[103] involved the computation of flow about a three-dimensional body of revolution at angle of attack. This configuration consisted of a cone-cylinder forebody with a conical afterbody and contained a centered, supersonic propulsive jet. Surface streamlines on the afterbody and density contours on the bilateral plane of symmetry are displayed in Fig. 16. For this computation the free-stream Mach number was 2.0, the jet exit Mach number was 2.5, the angle of attack was 6 deg, and the jet-to-free-stream pressure ratio was 3.0. The flow was turbulent with a Reynolds number based on cylinder diameter of 1.5 million, and turbulence was modeled with the Baldwin-Lomax model. This particular set of calculations is unique because of the complex data-base handling scheme utilized. The total data base associated with the 216,000 point grid was about 5 million words and was divided into a series of blocks each consisting of 8000 grid points. Manipulations of these blocks were performed us-

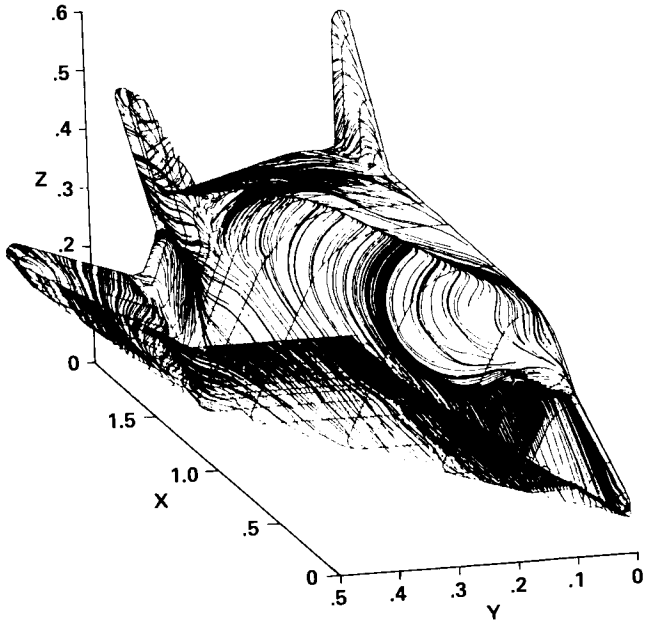


Fig. 13. Computed surface streamlines over the X-24C Lifting Body, $M_\infty = 5.95$, $\alpha = 6°$, $Re/m = 16.4$ x$10^6$, Shang and Scherr.[102]

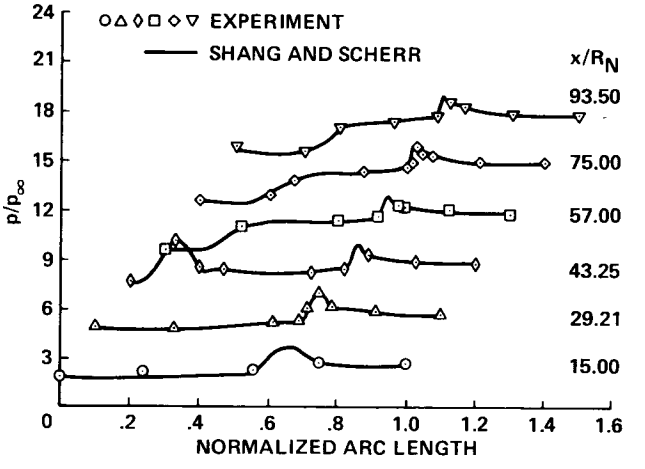


Fig. 14. Forebody pressure comparisons for the solution of Fig. 13, Shang and Scherr.[102]

ing the block data-base handling scheme described by Pulliam and Lomax.[104] With this approach very large grids were accomodated on a computer with a limited main memory for a flow field of considerable complexity.

The level of geometric complication, exhibited by the results from the preceeding paragraph and the section on transonic flow, has advanced rapidly during the past several years. However, a significant amount of work still remains. This area, along with turbulence modeling, was identified by Chapman[11,13] as one of the chief items pacing further development of computational aerodynamics. The key feature required to mature this area for three-dimensional applications is automation. Elements of this automation process must include surface grid generation,

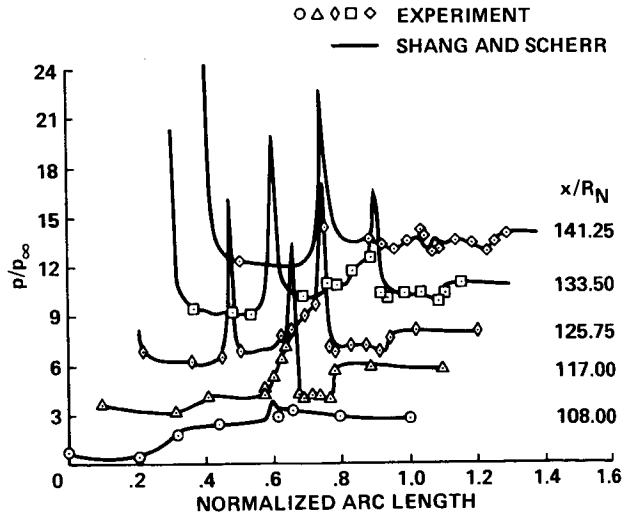


Fig. 15. Afterbody pressure comparisons for the solution of Fig. 13, Shang and Scherr.[102]

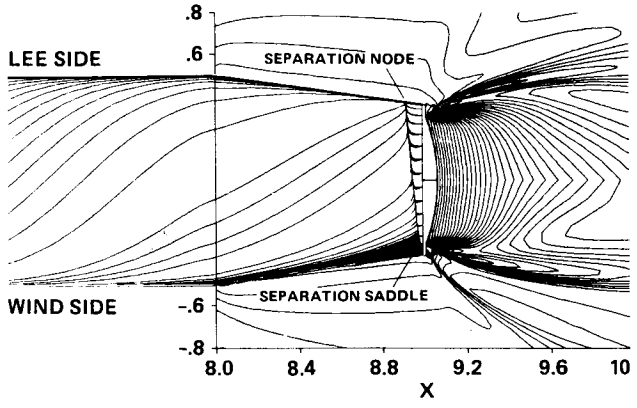


Fig. 16. Afterbody flow detail: surface streamlines and density contours on the bilateral plane of symmetry, $M_\infty = 2$, $M_J = 2.5$, $\alpha = 6°$, $P_J/P_\infty = 3$, $Re_D = 1.5\text{x}10^6$, Deiwert and Rothmund.[103]

zoning algorithms, and interior grid generation with solution adaptive capabilities. One possible alternative which may have a significant impact on the automation process is Artificial Intelligence as described by Andrews.[105] Progress in individual applications is anticipated to proceed at a fast rate, however, progress in automating the whole geometry and grid generation process will be slower to evolve.

A large amount of work associated with viscous supersonic flows has been completed using the PNS formulation. This includes the pioneering work on cones and blunt cones at angle of attack by Lin and Rubin,[106] Lubbard and Helliwell,[107] and Agarwal and Rakich;[108] the work on jets by McDonald and Briley;[109] and the work on ogive-cylinders by Rakich et al.[110] Applications of the PNS formulation to supersonic projectile aerodynamics have been presented by Schiff and Sturek[111] and Sturek and Schiff[112] using the formulation described in Schiff and Steger.[113] Sensitive magnus force calculations are reported and described in the Ref. 112.

Additional results utilizing the PNS formulation for more complicated geometries have been presented by Rai and Chaussee[114] and Rai et al.[115] for finned missles and projectiles, by Kaul and Chaussee[116] and Chaussee et al.[117] for the X-24C lifting body, by Chaussee et al.[118] for the Space Shuttle Orbiter, and by Chaussee et al.[119] and Wai et al.[120] for a generic supersonic-cruise fighter configuration. A typical result for the Space Shuttle Orbiter study of Ref. 118 is shown in Fig. 17. The free-stream Mach number for this calculation was 7.9, the angle of attack was 25 deg, and the Reynolds number was 2.4 million/m. Three-dimensional particle paths are displayed over the orbiter and show vortices forming on the leeside of the orbiter and at the wing/fuselage juncture. Another interesting PNS result is presented by Chaussee[17] for the blunt-nosed, biconic configuration displayed in Fig. 18. This configuration contained slices on both the windward and leeward sides and a control surface protrubing from the windward surface. The heat transfer distribution is

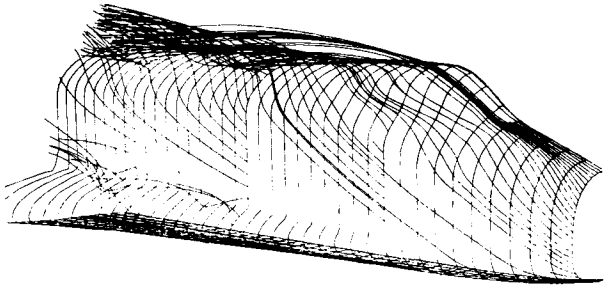

Fig. 17. Computed three-dimensional particle paths about the Space Shuttle Orbiter configuration, PNS formulation, $M_\infty = 7.9$, $\alpha = 25°$, $Re/m = 2.4\text{x}10^6$, Chaussee.[17]

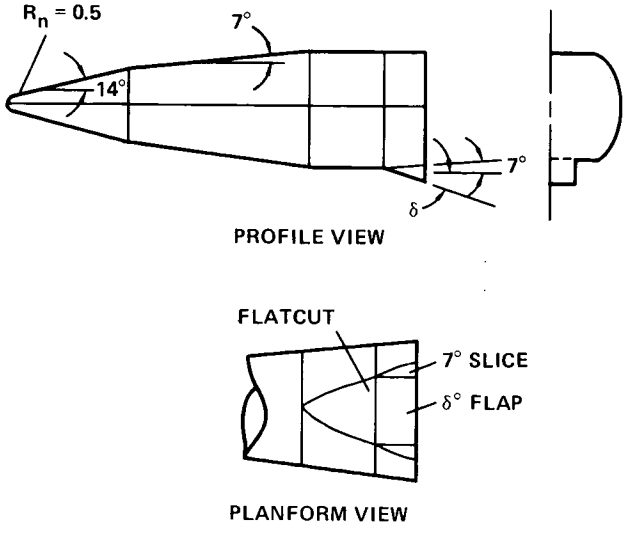


Fig. 18. Blunt biconic configuration with top and bottom slices and a flap control surface, Chaussee.[17]

compared with experiment along two meridinal planes in Fig. 19. The Mach number for this calculation was 10, the angle of attack was 10 deg and the Reynolds number was 0.3 million/m. Agreement is generally good with slight discrepancies caused by problems in predicting flow transition from laminar to turbulent.

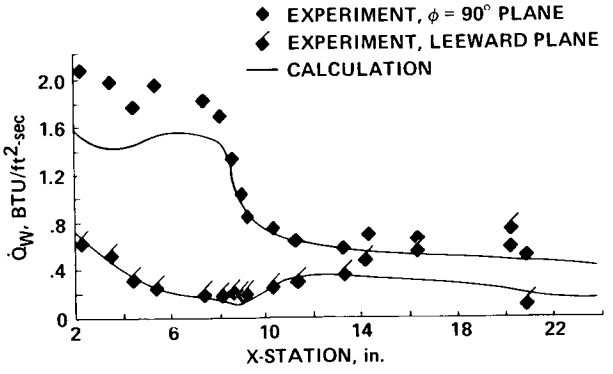


Fig. 19. Axial variation of the heat transfer over the biconic configuration in Fig. 18, PNS formulation, $M_\infty$ = 10, $\alpha = 10°$, $Re_D = 8.3\text{x}10^4$, Chaussee.[17]

## High-Alpha/Vortex-Dominated Flow Applications

The field of high-alpha flows has recently gained a lot of momentum in the CFD community. Early work with PNS applications has been complemented with emerging activities in the time-dependent RANS area. High-alpha flows are more difficult to understand and to compute because of several factors. First of all, associated with high-alpha flows are large vortex-dominated flow separations with complicated flow physics that are not well understood. Computing these flow fields accurately means predicting vortex formation in the boundary layer, the lift-off process, the vorticity transport process, and the vortex-vortex interaction process. Because a significant amount of flow detail can exist out of the boundary layer, providing the proper level of grid resolution in the proper places is more complicated. Secondly, high-alpha flows are generally unsteady in nature and can be wildly asymmetric even when the boundary conditions of the flow are essentially symmetric. Turbulence modeling is another difficulty associated with computing vortex-dominated flows. What turbulence models are appropriate for these flows, is a typically asked question which is largely unanswered to date. A good survey for high-alpha, vortex-dominated flows is given by Newsome and Kandil.[121]

Much of the work on the PNS fromulation presented above in the section on supersonic/hypersonic flow is intimately related to the field of high-alpha flow field studies. For high-alpha flows which are supersonic and which contain no streamwise separations, utilization of the PNS approach may be the most appropriate and certainly is more economical than the time-dependent RANS approach. Two examples that utilize this philosophy to study, in particular, high-alpha physics are given by Degani and Schiff[122] and Vigneron et al.[123] The results of Ref. 122 are interesting in that the standard Baldwin-Lomax turbulence model was modified for high angle-of-attack flows involving vortex lift off. The boundary layer thickness is computed from the vorticity distribution in the standard Baldwin-Lomax model. This quantity is inappropriately determined when vorticies lift off the surface. The Degani-Schiff modification fixes this difficulty and produces good agreement with experiment even for vortex lift off.

Computational work in the area of high-alpha flows has more recently centered on the use of the time-dependent RANS approach. Interesting examples in this area include Pulliam and Steger,[51] Kordulla et al.,[124] Obayashi et al.,[125] Aki and Yamada,[126] and Ying et al.[127] where solutions over hemisphere-cylinder configurations have been studied in the transonic and low-supersonic regime; Fujii and Kutler,[128,129] Rizzetta and Shang,[130] Pan and Pulliam,[131] Mehta,[132] and Chaderjian[133] where high-alpha flows over wings, delta-wings, yawed wings, and wing-strake combinations have been studied; and Newsome and Adams[134] where the vortical flow over elliptical bodies at high angles of attack have been studied.

Results from Refs. 127 and 134 are particularly striking and are displayed in Figs. 20 and 21, respectively. Figure 20 shows computed surface velocity vectors over a

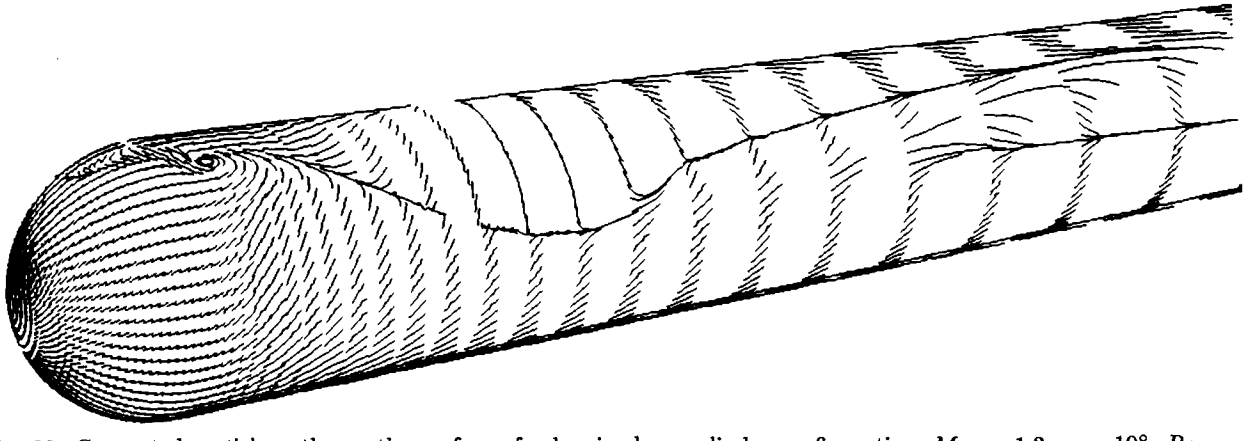

Fig. 20. Computed particle paths on the surface of a hemi-sphere-cylinder configuration, $M_\infty = 1.2$, $\alpha = 19°$, $Re_D = 4.45\text{x}10^5$, Ying et al.[127]

hemisphere-cylinder combination inserted into a Mach 1.2 stream at an angle of attack of 19 deg and a Reynolds number based on the cylinder diameter of 445,000. This calculation was laminar and therefore no turbulence model was used. The surface velocity vector pattern, which is in good agreement with the experimental oil flow, was computed with a new upwind algorithm described in Ref. 127

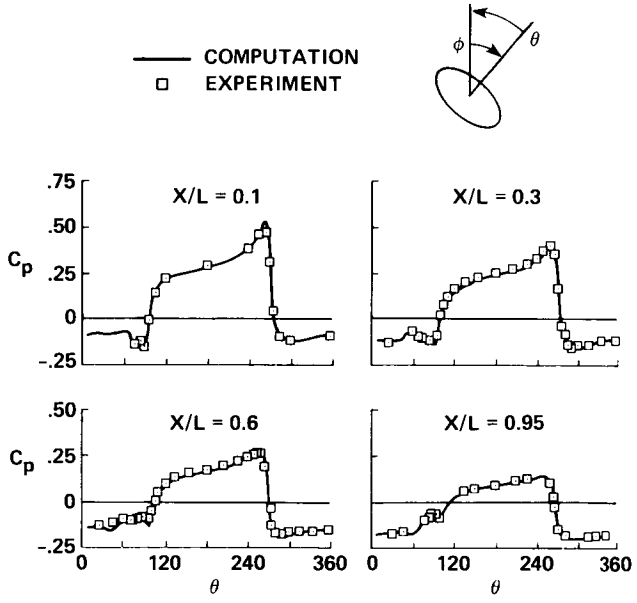


Fig. 21. Pressure coefficient comparisons for an elliptical lifting body with angles of attack ($\alpha$) and roll ($\phi$), $M_\infty = 2.5$, $\alpha = 20°$, $\phi = 45°$, $Re/m = 6.6\text{x}10^6$, Newsome and Adams.[134]

on a fine grid consisting of (60 x 50 x 60 =) 180,000 points. Figure 21 shows computed pressure results from Ref. 134 compared with experiment for the flow around an elliptical body. The Mach number for this calculation was 2.5; the angles of attack and roll were 20 and 45 deg, respectively; and the Reynolds number was 6.6 million/m. The numerical grid for this calculation was quite fine consisting of (35 x 101 x 61 =) 215,635 points. The explicit MacCormack method was used to integrate the RANS equations and a modified Baldwin-Lomax turbulence model was used to simulate turbulence. The excellent correlation of this calculation to experiment is obvious from Fig. 21. The reader is referred to additional interior flow field numerical/experimental comparisons, all in good agreement, in the original paper of Ref. 134.

Another set of results dealing with the computation of vortical flows is the work of Reznick and Flores[135] and Flores et al.[136] In these studies the previously mentioned TNS computer code was upgraded to include more complicated geometries. In particular, a modified F-16A configuration with a fared inlet and the tail removed was simulated with a zonal grid topology consisting of 16 grid zones. Particular emphasis in Ref. 135 was given to the study of the strake-leading-edge vortex. A comparison of computed wing pressures with experiment at a Mach number of 0.9, an angle of attack of 6 deg, and a Reynolds number of 6 million is shown in Fig. 22. The two results are in generally good agreement. The discrepancies in shock location and leading-edge pressure levels are perhaps due to coarse grid effects or the fact that the experimental data contained a flow-through inlet that was not modeled computationally. Details of the vortex formation at the strake leading edge for a Mach number of 0.6 and an angle of attack of 10 deg are shown in Figs. 23 and 24. Figure 23 shows a view of the modified F-16A with selected three-dimensional particle paths in the vicinity of the wing-root/strake juncture. Figure 24 shows a close-up view of the wing-root/strake juncture. From these two views, the formation of a vortex from both the strake and wing-root leading edges is obvious. The wing-root vortex draws the strake vortex beneath it and creates a strong spanwise flow toward the tip. This behavior is qualitatively displayed in experimental flow visualizations described in Ref. 135.

## Concluding Remarks

The numerical solution of the Navier-Stokes equations in three space dimensions has been reviewed. The areas of incompressible flow, transonic flow, supersonic/hypersonic flow, and high-alpha/vortex-dominated flow have all been considered. Applications research in all of these areas is seen to be increasing at an exponential rate. In addition, the geometrical complication of applications is advancing but at a slower rate. Areas which need concentrated attention in the near future are listed as follows:

1) Grid generation for complex geometries including surface grid generation, zoning algorithms, and solution adaptive grid concepts.

2) New developments in turbulence models for applications, especially those types of models that can be applied to obtain engineering answers for separated flow problems.

3) More complete CFD validation experiments which will allow more complete validation of CFD results and a physical assessement of why disagreements occur when they do occur.

4) More concentrated effort in the hypersonic flow regime including the development of sophisticated strong-shock capturing schemes, hypersonic turbulence models including the effects of transition, and the development of chemical equilibrium and nonequilibrium real-gas effects.

5) Convergence acceleration techniques for time-asymptotic problems, especially new algorithms which will lend themselves to vectorization and be efficient for new more sophisticated turbulence models and the more complicated physics associated with hypersonic flow.

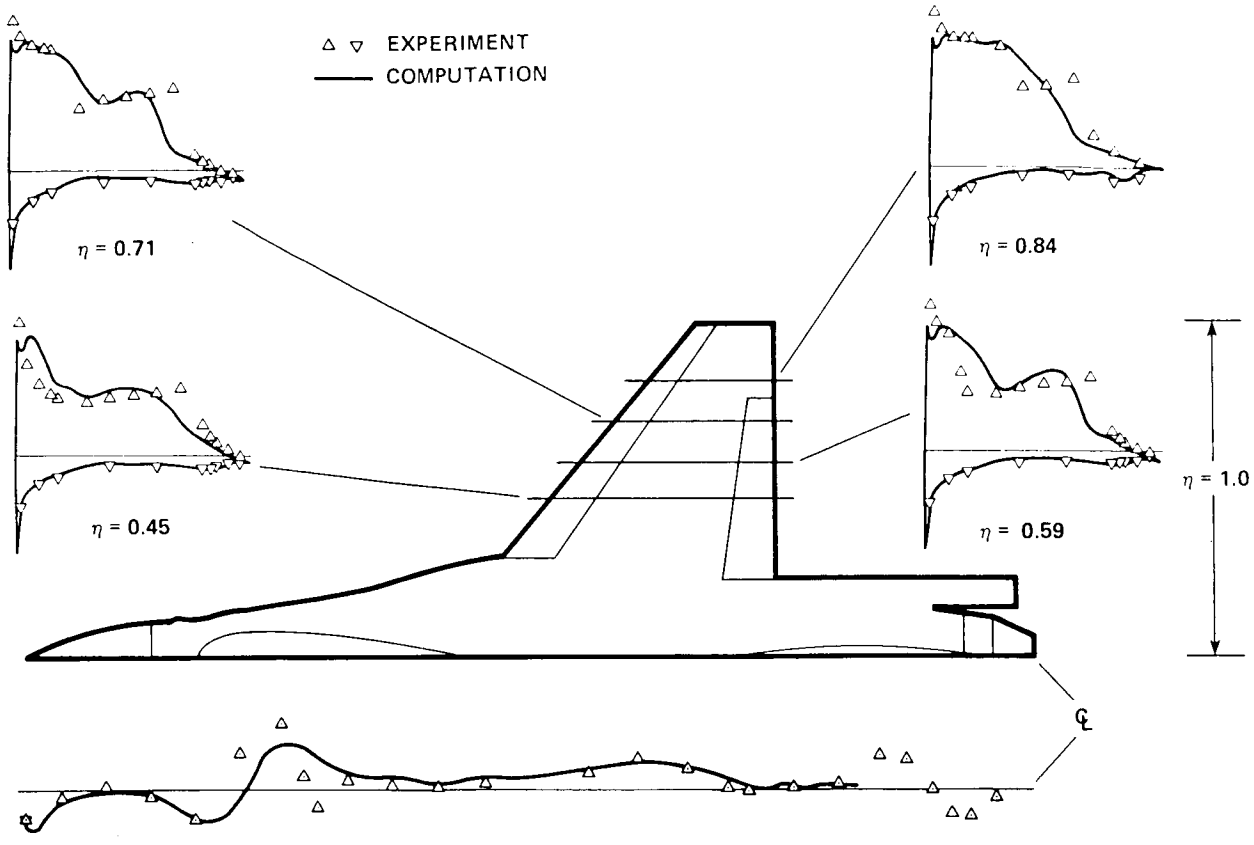


Fig. 22. Pressure coefficient comparisons on the wing and fuselage of a modified F-16A configuration, $M_\infty = 0.9$, $\alpha = 6.2°$, $Re_C = 4.5 \times 10^6$, Reznick and Flores.[135]

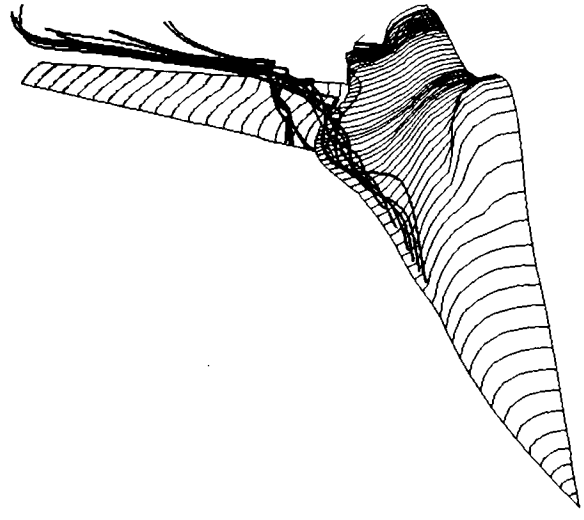

Fig. 23. Computed three-dimensional particle paths in the vicinity of a modified F-16A strake/wing juncture, $M_\infty = 0.6$, $\alpha = 10°$, Reznick and Flores.[135]

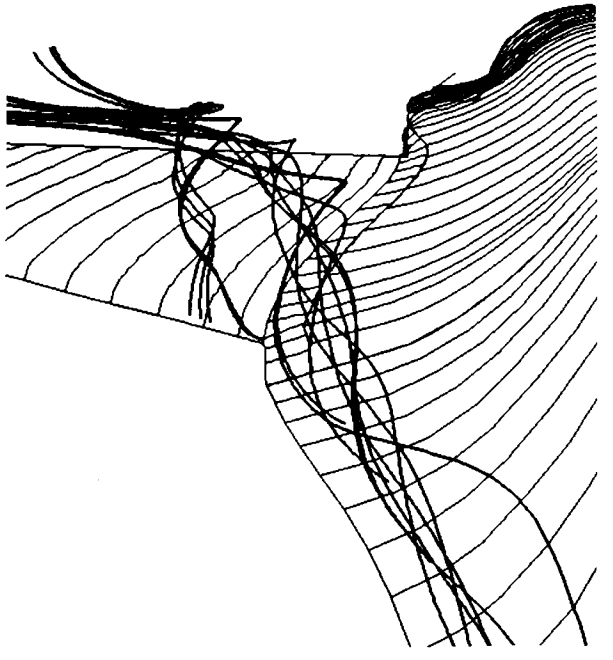

Fig. 24. Blow-up view of the three-dimensional particle paths shown in Fig. 23, Reznick and Flores.[135]

## References


[1]Peyret, R. and Viviand, H., "Computation of Viscous Compressible Flows Based on the Navier-Stokes Equations," AGARDograph No. 212, 1975.

[2] "The Influence of Computational Fluid Dynamics on Experimental Aerospace Facilities, A Fifteen Year Projection," Prepared by the Committee on Computational Aerodynamics Simulation Technology Developments, Aeronautics and Space Engineering Board, Commission on Engineering and Technical Systems, National Research Council, National Academy Press, Washington, D.C., 1983.

[3]Holst, T. L., Slooff, J. W., Yosihara, H., and Ballhaus, Jr., W.F., "Applied Computational Transonic Aerodynamics," AGARDograph No. 266, Aug. 1982.

[4]Holst, T. L., "Numerical Computation of Transonic Flow Governed by the Full Potential Equation," Presented at the 1983 VKI Lecture Series on Computational Fluid Dynamics in Brussels, Belgium, March 7-11, 1983; Also NASA TM-84310, Jan. 1983.

[5]Rogallo, R. S. and Moin, P., "Numerical Simulation of Turbulent Flows," Ann. Rev. Fluid Mechanics, Vol. 16, 1984, pp. 99-137.

[6]Baldwin, B. S. and Lomax, H., "Thin Layer Approximation and Algebraic Model for Separated Turbulent Flows," AIAA Paper No. 78-0257, Jan. 1978.

[7]Ballhaus, Jr., W. F., "Computational Aerodynamics and Supercomputers," Proceedings of the COMPCON 1984 28th IEEE Computer Society International Conference, Feb. 27-Mar. 1, 1984, pp. 3-14, IEEE Computer Society, Silver Spring, MD.

[8]Peterson, V. L., Ballhaus, Jr., W. F., and Bailey F. R., "Numerical Aerodynamic Simulation (NAS)," Large Scale Scientific Computation, Academic Press, 1984, pp. 215-236.

[9]Peterson, V. L., "A New Opportunity for Rotorcraft Technology," Presented at the American Helicopter Society 42nd Annual Forum and Technology Display, June 1986.

[10]Kutler, P., "A Perspective of Computational Fluid Dynamics," NASA TM 88246, May 1986.

[11]Chapman, D. R., "Computational Aerodynamics-Development and Outlook," AIAA J., Vol. 17, No. 12, Dec. 1979, pp. 1293-1313.

[12]Anderson, D. A., Tannehill, J. C., and Pletcher, R. H., Computational Fluid Mechanics and Heat Transfer, Hemisphere Publishing Corp., Washington, 1984.

[13]Chapman, D. R., "Trends and Pacing Items in Computational Aerodynamics," Lecture Notes in Physics, Vol. 141, Eds. Reynolds, W. C. and MacCormack, R., Springer-Verlag, Berlin Heidelberg, Germany, 1981.

[14]Kutler, P., "A Perspective of Theoretical and Applied Computational Fluid Dynamics," AIAA J., Vol. 23, No. 3, Mar. 1985, pp. 328-341.

[15]Shang, J. S., "An Assessment of Numerical Solutions of the Compressible Navier-Stokes Equations," J. of Aircraft, Vol. 22, No. 5, May 1985, pp. 353-370.

[16]Mehta, U. and Lomax, H., "Reynolds-Averaged Navier-Stokes Computations of Transonic Flows–the State of the Art," In Transonic Aerodynamics, Ed. Nixon, D., Vol. 81, Progress in Astronautics and Aeronautics, 1982, pp. 297-375.

[17]Chaussee, D. S., "High Speed Viscous Flow Calculations About Complex Configurations, NASA TM 88237, April 1986.

[18]Orszag, S. A. and Israeli, M., "Numerical Simulation of Viscous Incompressible Flows," Annual Review of Fluid Mechanics, Vol. 6, 1974, pp. 281-318.

[19]Turkel, E., "Progress in Computational Physics," ICASE Report No. 82-23, Aug. 1982.

[20]Thompson, J. F., "Grid Generation Techniques in Computational Fluid Dynamics," AIAA J., Vol. 22, No. 11, Nov. 1984, pp. 1505-1523.

[21]Lakshminarayana, B., "Turbulence Modeling for Complex Flows," AIAA Paper No. 85-1652, July 1985.

[22]Marvin, J. G., "Future Requirements of Wind Tunnels for Computational Fluid Dynamics Code Verification," AIAA Paper No. 86-0752-CP, Jan. 1986.

[23]Harlow, F. H. and Welch, J. E., "Numerical Calculation of Time-Dependent Viscous Incompressible Flow with Free Surface," Physics of Fluids, Vol. 8, Dec. 1965, pp. 2182-2189.

[24]Chorin, A. J., "A Numerical Method for Solving Incompressible Viscous Flow Problems," J. Comp. Phys., Vol. 2, 1967, pp. 12-26.

[25]Patankar, S. V. and Spalding, D. B., "A Calculation Procedure for Heat, Mass and Momentum Transfer in Three-Dimensional Parabolic Flows," Int. J. Heat Mass Transfer, Vol. 15, 1972, pp. 1787-1806.

[26]Briley, W. R., "Numerical Method for Predicting Three Dimensional Flows in Ducts," J. Comp. Phys., Vol. 14, No. 1, 1974, pp. 8-28.

[27]Ghia, K. N. and Sokhey, J. S., "Laminar Incompressible Viscous Flow in Curved Ducts of Regular Cross-Sections," J. of Fluids Engr., Vol. 99, 1977, pp. 640-648.

[28]Ghia, U., Ghia, K. N., and Studerus, C. J., "Three-Dimensional Laminar Incompressible Flow in Straight Polar Ducts," Int. J. of Comp. and Fluids, Vol. 5, No. 4, 1977, pp. 205-218.

[29]Buggeln, R. C., Briley, W. R., and McDonald, H., "Solution of the Navier-Stokes Equations for Three-Dimensional Turbulent Flow with Viscous Sublayer Resolution," AIAA Paper No. 81-1023, June 1981.

[30]Ghia, U., Ghia, K. N., and Goyal, R. K., "Three-Dimensional Viscous Incompressible Flow in Curved Polar Ducts," AIAA Paper No. 81-1455, June 1981.

[31]Pouagare, M. and Lakshimarayana, B., "A Space-Marching Method for Viscous Incompressible Internal Flows," J. Comp. Phys., Vol. 64, No. 2, June 1986, pp. 389-415.

[32]Roberts, D. W. and Forester, C. K., "Parabolic Procedure for Flows in Ducts with Arbitrary Cross Sections," AIAA J., Vol. 17, No. 1, Jan. 1979, pp. 33-40.

[33]Himeno, R., Shirayama, S., Kamo, K., and Kuwahara, K., "Computational Study of Three-Dimensional Wake Structure," AIAA Paper No. 85-1617, July 1985.

[34]Kawamura, T. and Kuwahara, K., "Computation of High Reynolds Number Flow around a Circular Cylinder with Surface Roughness," AIAA Paper No. 84-0340, Jan. 1984.

[35]Kwak, D., Chang, J. C., Shanks, S., Chakravarthy, S. R., "A Three-Dimensional Incompressible Navier-Stokes Flow Solver Using Primitive Variables," AIAA J., Vol. 24, No. 3, March 1986, pp. 390-396.

[36]Gorski, J., Govindan, T., and Lakshiminarayana, B., "Computation of Three-Dimensional Turbulent Shear Flows in Corners," AIAA Paper No. 83-1733, July 1983.

[37]Chang, J. L. C., Kwak, D., Dao, S. C., and Rosen, R., "A Three-Dimensional Incompressible Flow Simulation Method and Its Application to the Space Shuttle Main Engine, Part I - Laminar Flow," AIAA Paper No. 85-0175, Jan. 1985.

[38]Chang, J. L. C., Kwak, D., Dao, S. C., and Rosen, R., "A Three-Dimensional Incompressible Flow Simulation Method and Its Application to the Space Shuttle Main Engine, Part II - Turbulent Flow," AIAA Paper No. 85-1670, July 1985.

[39]Ziebarth, J. P., Barson, S., and Rosen, R., "Computational Fluid Dynamics as a Design Tool for Hot Gas Manifold of the Space Shuttle Main Engine," Institute for Computational Studies, Report No. 86002, Jan. 1986.

[40]Kwak, D., Rogers, S., Kaul, U. K., and Chang, J. L. C., "A Numerical Study of Incompressible Juncture Flows," NASA TM 88319, Aug. 1986.

[41]Rogers, S. E., Kwak, D., and Kaul, U. K., "A Numerical Study of Three-Dimensional Incompressible Flow Around Multiple Posts," AIAA Paper No. 86-0353, Jan. 1986.

[42]Chang J. L. C., and Kwak, D., "On the Method of Pseudo Compressibility for Numerically Solving Incompressible Flows," AIAA Paper No. 84-0252, Jan. 1984.

[43]Steger, J. L. and Kutler, P., "Implicit Finite-Difference Procedures for the Computation of Vortex Wakes," AIAA J., Vol. 15, No. 4, April 1977, pp. 581-590.

[44]Rogers, S. E., Chang, J. L. C., and Kwak, D., "A Diagonal Algorithm for the Method of Pseudo Compressibility," AIAA Paper No. 86-1060, May 1986.

[45]Beam, R. M. and Warming, R. F., "An Implicit Finite-Difference Algorthm for Hyperbolic Systems in Con servation-Law Form," J. Comp. Phys., Vol. 22, No. 1, 1976, pp. 87-110.

[46]Briley, W. R. and McDonald, H., "Solution of the Multidimensional Compressible Navier-Stokes Equations by a Generalized Implicit Method," J. Comp. Phys., Vol. 24, No. 4, 1977, pp. 372-397.

[47]MacCormack, R. W., "A Numerical Method for Solving the Equations of Compressible Viscous Flow," AIAA J., Vol. 20, No. 9, Sept. 1982, pp. 1275-1281.

[48]MacCormack, R. W., "The Effect of Viscosity in Hypervelocity Impact Cratering," AIAA Paper No. 69-354, April 1969.

[49]Mansour, N. N., "Numerical Simulation of the Tip Vortex Off a Low-Aspect Ratio Wing at Transonic Speed," AIAA Paper No. 84-0522, Jan. 1984.

[50]Hinson, B. L. and Burdges, K. P., "Acquisition and Application of Transonic Wing and Far-Field Test Data for Three-Dimensional Computational Method Evaluation," Report No. AFOSR-TR-80-0421, Lockheed Georgia Co. Marietta, Ga., 1980.

[51]Pulliam, T. H. and Steger, J. L., "Implicit Finite-Difference Simulations of Three-Dimensional Compressible Flow," AIAA Paper 78-10, Jan. 1978. Also AIAA J., Vol. 18, No. 2, Feb. 1980, pp. 159-167.

[52]Agarwal, R. K. and Deese, J. E., "Computation of Transonic Viscous Airfoil, Inlet and Wing Flowfields," MDRL Report No. 84-29, June 1984.

[53]Jameson, A., Schmidt, W., and Turkel, E., "Numerical Solution of the Euler Equations by Finite Volume Methods Using Runge-Kutta Time-Stepping Schemes," AIAA Paper No. 81-1259, July 1981.

[54]Schmit, V. and Charpin, F., "Pressure Distributions on the ONERA-M6 Wing at Transonic Mach Numbers," AGARD Report AR-138, May 1979.

[55]Holst, T. L., Kaynak, U., Gundy, K. L., Thomas, S. D., Flores, J., and Chaderjian, N., "Numerical Solution of Transonic Wing Flows Using an Euler/Navier-Stokes Zonal Approach," AIAA Paper No. 85-1640, July 1985.

[56]Flores, J., "Convergence Acceleration for a Three-Dimensional Euler/Navier-Stokes Zonal Approach," AIAA Paper 85-1495, July 1985.

[57]Kaynak, U., Holst, T. L., Cantwell, B. J., and Sorenson, R. L., "Numerical Simulation of Transonic Separated Flows over Low Aspect Ratio Wings," AIAA Paper No. 86-0508, Jan. 1986.

[58]Kaynak, U., Holst, T. L., and Cantwell, B. J., "Computation of Transonic Separated Wing Flows Using an Euler/Navier-Stokes Zonal Approach," NASA TM 88311, July 1986.

[59]Srinivasan, G. R., McCroskey, W. J., Baeder, J. D., and Edwards, T. A., "Numerical Simulation of Tip Vorticies of Wings in Subsonic and Transonic Flows," AIAA Paper No. 86-1095, May 1986.

[60]Pulliam, T. H. and Chaussee, D. S., "A Diagonal Form of an Implicit Approximate-Factorization Algorithm," J. Comp. Phys., Vol. 39, No. 2, Feb. 1981, pp. 347-363.

[61]Lockman, W. K. and Seegmiller, H. L., "An Experimental Investigation of the Subcritical and Supercritical Flow About a Swept Semispan Wing," NASA TM-84367, June 1983.

[62]Keener, E. R., "Computational-Experimental Pressure Distributions on a Transonic low-Aspect-Ratio Wing," AIAA Paper No. 84-2092, Aug. 1984.

[63]Keener, E. R., "Boundary-Layer Measurements on a Transonic Low-Aspect Ratio Wing," NASA TM-88214, May 1986.

[64]Obayashi, S. and Fujii, K., "Computation of Three-Dimensional Viscous Transonic Flows with the LU Factored Scheme," AIAA Paper No. 85-1510, July 1985.

[65]Fujii, K. and Obayashi, S., "Practical Applications of New LU-ADI Scheme for the Three-Dimensional Navier-Stokes Computation of Transonic Viscous Flows," AIAA Paper No. 86-0513, Jan. 1986.

[66]Steger, J. L. and Warming, R. F., "Flux Vector Splitting of the Inviscid Gasdynamic Equations with Application to Finite-Difference Methods," J. Comp. Phys., Vol. 40, 1981, pp. 263-293.

[67]Lombard, C. K., Bardina, J., Venkatapathy, E., and Oliger, J., "Multi-Dimensional Formulation of CSCM - An Upwind Flux Difference Eignevector Split Method for the Compressible Navier-Stokes Equations," AIAA Paper No. 83-1895, July 1983.

[68]Fujii, K. and Obayashi, S., "Navier-Stokes Simulation of Transonic Flow over Wing-Fuselage Combina-

tions," AIAA Paper No. 86-1831, June 1986.

[69]Vadyak, J., "Simulation of Transonic Three-Dimensional Nacelle/Inlet Flowfields Using an Euler/Navier-Stokes Algorithm," AIAA Paper No. 85-0084, Jan. 1985.

[70]Swisshelm, J. M. and Johnson, G.M., "Numerical Simulation of Three-Dimensional Flowfields Using the CYBER 205," Inst. for Comp. Studies, ICS Technical Report 85002, Nov. 1984.

[71]Chaussee, D. S., Buning, P. G., and Kirk, D. B., "Convair 990 Transonic Flow-Field Simulation About the Forward Fuselage," AIAA Paper No. 83-1785, July 1983.

[72]Cosner, R., "Relaxation Solution for Viscous Transonic Flow about Fighter-Type Forebodies and Afterbodies," AIAA Paper No. 82-0252, Jan. 1982.

[73]Deiwert, G. S., "Numerical Simulation of Three-Dimensional Boattail Afterbody Flow Field," AIAA Paper No. 80-1347, July 1980.

[74]Purohit, S. C., Shang, J. S., and Hankey, Jr., W. L., "Numerical Simulation of Flow Around a Three-Dimensional Turret," AIAA Paper No. 82-1020, June 1982.

[75]Purohit, S. C., Shang, J. S., and Hankey, Jr., W. L., "Effect of Suction on the Wake Structure of a Three-Dimensional Turret," AIAA Paper No. 83-1738, July 1983.

[76]Nietubicz, C. J., Sturek, W. B., and Heavey, K. R., "Computations of Projectile Magnus Effect at Transonic Velocities," AIAA Paper No. 83-0237, Jan. 1983.

[77]Nietubicz, C. J., Mylin, D. C., and Sahu, J., "Aerodynamic Coefficient Predictions for a Projectile Configuration at Transonic Speeds," AIAA Paper No. 84-0326, Jan. 1984.

[78]Sahu, J., Nietubicz, C. J., and Steger, J., "Navier-Stokes Computations of Projectile Base Flow With and Without Base Injection," AIAA Paper No. 83-0224, Jan. 1983.

[79]Li, C. P., "A Numerical Study of Laminar Flow Separation on Blunt Flared Cones at Angle of Attack," AIAA Paper No. 74-585, June 1974.

[80]Holst, T. L. and Tannehill, J. C., "Numerical Computation of Three-Dimensional Blunt Body Flow Fields with an Impinging Shock," Iowa State University, Engineering Research Institute, Report No. ISU-ERI-Ames-75169, July 1975.

[81]Shang, J. S. and Hankey, W. L., "Numerical Solution of the Compressible Navier-Stokes Equations for a Three-Dimensional Corner," AIAA J., Vol. 15, No. 11, Nov. 1977, pp. 1575-1582.

[82]Hung, C. M. and MacCormack, R. W., "Numerical Solution of Supersonic Laminar Flow over a Three-Dimensional Compression Corner," AIAA Paper No. 77-694, June 1977.

[83]Hung, C. M., "Numerical Solution of Supersonic Laminar Flow Over an Inclined Body of Revolution," AIAA Paper No. 79-1547, July 1979.

[84]Hung, C. M., "Impingement of an Oblique Shock Wave on a Cylinder," J. of Spacecraft and Rockets, Vol. 23, No.6, May-June 1983, pp. 201-206.

[85]Knight, D. D., "A Hybrid Explicit-Implict Numerical Algorithm for the Three-Dimensional Compressible Navier-Stokes Equations," AIAA Paper No. 83-0223, Jan. 1983.

[86]Hung, C. M. and MacCormack, R. W., "Numerical Solution of Three-Dimensional Shock Wave and Turbulent Boundary-Layer Interaction," AIAA J., Vol. 16, No. 10, Oct. 1978, pp. 1090-1096.

[87]Hung, C. M. and Kordulla, W., "A Time-Split Finite-Volume Algorithm for Three-Dimensional Flow-Field Simulation," AIAA J., Vol. 22, No. 11, Nov. 1984, pp. 1564-1572.

[88]Hung, C. M. and Buning, P., "Simulation of Blunt-Fin-Induced Shock Wave and Turbulent Boundary-Layer Interaction," J. Fluid Mechanics, Vol. 154, May 1985, pp. 163-185.

[89]Horstman, C. C., Kussoy, I., and Lockman, W. K., "Computation of Three-Dimensional Shock-Wave/Turbulent Boundary-Layer Interaction Flows," Proceedings of the Third Symposium on Numerical and Physical Aspects of Aerodynamic Flows, Long Beach, CA, Jan 1985.

[90]Horstman, C. C., "A Computational Study of Complex Three-Dimensional Compressible Turbulent Flowfields," AIAA J., Vol. 23, No. 10, Oct. 1985, pp. 1461-1462.

[91]Knight, D., "Numerical Simulation of 3-D Shock Turbulent Boundary Layer Interaction Generated by a Sharp Fin," AIAA J., Vol. 23, No. 12, Dec. 1985, pp. 1885-1891.

[92]Knight, D., Horstman, C., Shapey, B., and Bodnonoff, S., "The Flowfield Structure of the 3-D Shock Wave-Boundary Layer Interaction Generated by a 20 deg Sharp Fin at Mach 3," AIAA Paper No. 86-0343, Jan. 1986.

[93]Horstman, C., "Computation of Sharp-Fin-Induced Shock Wave/Turbulent Boundary-Layer Interactions," AIAA J., Vol. 24, No. 9, Sept. 1986, pp. 1433-1440.

[94]Jones, W. P. and Launder, B. E., "The Prediction of Laminarization with Two-Equation Model of Turbulence," Inter. J. of Heat and Mass Transfer, Vol. 15, Feb. 1972, pp. 301-314.

[95]Viegas, J. R. and Rubesin, M. W., "Wall-Function Boundary Conditions in the Solution of the Navier-Stokes Equations for Complex Compressible Flows," AIAA Paper No. 83-1694, July 1983.

[96]Shang, J. S., "Numerical Simulation of Wing-Fuselage Interference," AIAA Paper No. 81-0048, Jan. 1981.

[97]Shang, J. S., "Numerical Simulation of Wing-Fuselage Aerodynamic Interaction," AIAA Paper No. 83-0225, Jan. 1983.

[98]Kumar, A. J., "Numerical Simulation of Flow Through Scramjet Inlets Using a Three-Dimensional Navier-Stokes Code," AIAA Paper No. 85-1664, July 1985.

[99]Howlett, D. G. and Hunter, L. G., "A Study of a Supersonic Axisymmetric Spiked Inlet at Angle of Attack Using the Three-Dimensional Navier-Stokes Equations," AIAA Paper No. 86-0308, Jan. 1986.

[100]Rizk, Y. M. and Ben-Shmuel, S., "Computation of the Viscous Flow Around the Shuttle Orbiter at Low Supersonic Speeds," AIAA Paper No. 85-0168, Jan. 1985.

[101]Li, C. P., "Numerical Procedure for Three-Dimensional Hypersonic Viscous Flow Over Aerobrake Configurations," Proceedings of the Inter. Sym. on Comp. Fluid Dynamics, Tokyo, Japan, Sept. 1985, pp. 833-844.

[102]Shang, J. S. and Scherr, S. J., "Navier-Stokes Solution of the Flow Field Around a Complete Aircraft," AIAA Paper No. 85-1509, July 1985.

[103]Deiwert, G. S. and Rothmund, H., "Three-Dimensional Flow Over a Conical Afterbody Containing a Centered Propulsive Jet: A Numerical Simulation," AIAA Paper No. 83-1709, July 1983.

[104]Lomax, H. and Pulliam, T. H., "A Fully Implicit Factored Code for Computing Three-Dimensional Flows on the ILLIAC IV," Parallel Computations, G. Rodrigue, Ed., Academic Press, New York, 1982, pp. 217-250.

[105]Andrews, A. E., "Progress and Challenges in the Application of Artificial Intelligence to Computational Fluid Dynamics," AIAA Paper No. 87-0593, Jan. 1987.

[106]Lin, T. C. and Rubin, S. G., "Viscous Flow Over a Cone at Moderate Incidence: I - Hypersonic Tip Region," Inter. J. of Comp. and Fluids, Vol. 1, 1973, pp. 37-57.

[107]Lubbard, S. C. and Helliwell, W. S., "Calculation of the Flow on a Cone at High Angle of Attack," AIAA J., Vol. 12, No. 7, July 1974, pp. 965-974.

[108]Agarwal, R. and Rakich, J. V., "Computation of Hypersonic Laminar Viscous Flow Past Spinning Sharp and Blunt Cone at High Angle of Attack," AIAA Paper No. 78-65, Jan. 1978.

[109]McDonald, H. and Briley, W., "Three-Dimensional Supersonic Flow of a Viscous or Inviscid Gas," J. Comp. Phys., Vol. 19, No. 2, Oct. 1975, pp. 150-178.

[110]Rakich, J. V., Vigneron, Y.C., and Agarwal, R., "Computation of Supersonic Viscous Flows Over Ogive-Cylinders at Angle of Attack," AIAA Paper No. 79-0131, Jan. 1979.

[111]Schiff, L. B. and Sturek, W. B., "Numerical Simulation of Steady Supersonic Flow Over an Ogive-Cylinder-Boattail Body," AIAA Paper No. 80-0066, Jan. 1980.

[112]Sturek, W. B. and Schiff, L. B., "Computations of the Magnus Effect for Slender Bodies in Supersonic Flow," AIAA Paper No. 80-1586, Aug. 1980.

[113]Schiff, L. B. and Steger, J. L., "Numerical Simulation of Steady Supersonic Viscous Flow," AIAA Paper No. 79-0130, Jan. 1979.

[114]Rai, M. M. and Chaussee, D. S., "New Implicit Boundary Procedures: Theory and Applications," AIAA Paper No. 83-0123, Jan. 1983.

[115]Rai, M. M., Chaussee, D. S., and Rizk, Y., "Calculation of Viscous Supersonic Flows over Finned Bodies," AIAA Paper No. 83-1667, July 1983.

[116]Kaul, U. and Chaussee, D. S., "A Comparative Study of the Parabolized Navier-Stokes (PNS) Code Using Various Grid Generation Techniques," AIAA Paper No. 84-0459, Jan. 1984.

[117]Chaussee, D. S., Patterson, J. L., Kutler, P., Pulliam, T. H., and Steger, J. L., "A Numerical Simulation of Hypersonic Flows over Arbitrary Geometries at High Angle of Attack," AIAA Paper No. 81-0050, Jan. 1981.

[118]Chaussee, D. S., Rizk, Y. M., and Buning, P. G., "Viscous Computations of a Space Shuttle Flowfield," Lecture Notes in Physics, Ninth International Conference on Numerical Methods in Fluid Dynamics, Vol. 218, 1984, pp. 148-153.

[119]Chaussee, D. S., Blom, G., and Wai, J. C., "Numerical Simulation of Viscous Supersonic Flow Over a Generic Fighter Configuration," NASA TM-86823, Dec. 1985.

[120]Wai, J. C., Blom, G., and Yoshihara, H., "Calculations for a Generic Fighter at Supersonic High-Lift Conditions," AGARD Fluid Dynamics Panel Symposium on Applications of Computational Fluid Dynamics in Aeronautics, France, April 1986.

[121]Newsome, R. W. and Kandil, O. A., "Vortex Flow Aerodynamics - Physical Aspects and Numerical Simulation," AIAA Paper No. 87-0205, Jan. 1987.

[122]Degani, D. and Schiff, L. B., "Computation of Supersonic Viscous Flows Around Pointed Bodies at Large Incidence," AIAA Paper No. 83-0034, Jan. 1983.

[123]Vigneron, Y. C., Rakich, J. V., and Tannehill, J. C., "Calculation of Supersonic Viscous Flow over Delta Wings with Sharp Subsonic Leading Edges," AIAA Paper No. 78-1137, July 1978.

[124]Kordulla, W., Vollmers, H., and Dallmann, U., "Simulation of Three-Dimensional Transonic Flow with Separation Past a Hemisphere-Cylinder Configuration," AGARD CPP-412, Appls. of Comp. Fluid Dynamics in Aero., Paper 31, April 1986.

[125]Obayashi, S. and Fujii, K., "Computation of Three-Dimensional Viscous Transonic Flows with the LU Factored Scheme," AIAA Paper No. 85-1510, July 1985.

[126]Aki, T. and Yamada, S., "A Supercomputer Simulation of Three Dimensional Viscous Flow," Proceeding of the Inter. Sym. on Comp. Fluid Dynamics, Sept. 1985, Tokyo, Japan, pp. 821-832.

[127]Ying, S. X., Steger, J. L., Schiff, L., and Baganoff, D., "Numerical Simulation of Unsteady, Viscous, High-Angle-of-Attack Flows Using a Partially Flux-Split Algorithm," AIAA Paper No. 86-2179, Aug. 1986.

[128]Fujii, K. and Kutler, P., "Numerical Simulation of the Leading-Edge Separation Vortex for a Wing and Strake-Wing Configuration," AIAA Paper No. 83-1908, July 1983.

[129]Fujii, K. and Kutler, P., "Numerical Simulation of the Viscous Flow Fields Over Three-Dimensional Complicated Geometries," AIAA Paper No. 84-1550, June 1984.

[130]Rizzetta, D. P. and Shang, J. S., "Numerical Simulation of Leading Edge Vortex Flows," AIAA Paper No. 84-1544, June 1984.

[131]Pan, D. and Pulliam, T. H., "The Computation of Steady Three-Dimensional Separated Flows over Aerodynamic Bodies at Incidence and Yaw," AIAA Paper No. 86-0109, Jan. 1986.

[132]Mehta, U., "The Computation of Flow Past an Oblique Wing Using the Thin-Layer Navier-Stokes Equations," NASA TM-88317, June 1986.

[133]Chaderjian, N. M., "Transonic Navier-Stokes Wing Solutions Using a Zonal Approach: Part 2. High Angle-of-Attack Simulation," Presented at the AGARD meeting in Aix En Provence, France, April 7-10, 1986; Also, NASA TM-88248, April 1986.

[134]Newsome, R. W. and Adams, M. S., "Numerical Simulation of Vortical-Flow Over an Elliptical-Body Missile at High Angles of Attack," AIAA Paper No. 86-0559, Jan. 1986.

[135]Reznick, S. G. and Flores, J., "Strake Generated Vortex Interactions for a Fighter-Like Configuration," AIAA Paper No. 87-0589, Jan. 1987.

[136]Flores, J., Reznick, S. G., Holst, T.L., and Gundy, K., "Transonic Navier-Stokes Solutions for a Fighter-Like Configuration," AIAA Paper No. 87-0032, Jan. 1987.